Organization of Visual Mossy Fiber Projections and Zebrin Expression in the Pigeon Vestibulocerebellum

Janelle M.P. Pakan,[2] David J. Graham,[2] and Douglas R. Wylie[1,2]*
[1]Department of Psychology, University of Alberta, Edmonton, Alberta, Canada, T6G 2E9
[2]Centre for Neuroscience, University of Alberta, Edmonton, Alberta, Canada, T6G 2E9

ABSTRACT

Extensive research has revealed a fundamental organization of the cerebellum consisting of functional parasagittal zones. This compartmentalization has been well documented with respect to physiology, biochemical markers, and climbing fiber afferents. Less is known about the organization of mossy fiber afferents in general, and more specifically in relation to molecular markers such as zebrin. Zebrin is expressed by Purkinje cells that are distributed as a parasagittal array of immunopositive and immunonegative stripes. We examined the concordance of zebrin expression with visual mossy fiber afferents in the vestibulocerebellum (folium IXcd) of pigeons. Visual afferents project directly to folium IXcd as mossy fibers and indirectly as climbing fibers via the inferior olive. These projections arise from two retinal recipient nuclei: the lentiformis mesencephali (LM) and the nucleus of the basal optic root (nBOR). Although it has been shown that these two nuclei project to folium IXcd, the detailed organization of these projections has not been reported. We injected anterograde tracers into LM and nBOR to investigate the organization of mossy fiber terminals and subsequently related this organization to the zebrin antigenic map. We found a parasagittal organization of mossy fiber terminals in folium IXcd and observed a consistent relationship between mossy fiber organization and zebrin stripes: parasagittal clusters of mossy fiber terminals were concentrated in zebrin-immunopositive regions. We also describe the topography of projections from LM and nBOR to the inferior olive and relate these results to previous studies on the organization of climbing fibers and zebrin expression. J. Comp. Neurol. 518:175–198, 2010.

INDEXING TERMS: zebrin; cerebellum; mossy fibers; compartmentation; vestibulocerebellum; lentiformis mesencephali; nucleus of the basal optic root; optokinetic

The fundamental architecture of the cerebellar cortex consists of parasagittal compartments that have been revealed by using anatomical, electrophysiological, and histological techniques (e.g., Voogd and Bigaré, 1980). Studies have shown that parasagittal zones can be defined by climbing fiber (CF) input, Purkinje cell efferents, and Purkinje cell response properties (Voogd, 1967; Oscarsson, 1969; Andersson and Oscarsson, 1978a,b; Voogd and Bigaré, 1980; Llinas and Sasaki, 1989; Sato and Kawasaki, 1991; De Zeeuw et al., 1994; Wylie et al., 1994, 1995, 2003a; Voogd and Glickstein, 1998; Ruigrok, 2003; Winship and Wylie, 2003; Sugihara and Shinoda, 2004; Voogd and Wylie, 2004; Apps and Garwicz, 2005). Fewer anatomical studies have also investigated this parasagittal organization in relation to mossy fiber (MF) input, with particular focus on the topographical organization of somatosensory afferents to the cerebellar cortex from spinocerebellar and cuneocerebellar pathways (Voogd et al., 1969; Ekerot and Larson, 1973; Matsushita et al., 1984; Gerrits et al., 1985; Arends and Zeigler, 1989; Matsushita et al., 1991; Akintunde and Eisenman, 1994; Ji and Hawkes, 1994).

Compartmentation of the cerebellar cortex has also been revealed immunohistochemically with several molecular markers (for review, see Hawkes and Gravel, 1991; Herrup and Kuemerle, 1997), but the most thoroughly studied of these is zebrin II (aldolase C; Brochu et al., 1990;

Additional Supporting Information may be found in the online version of this article.

Grant sponsor: the Canadian Institute for Health Research (CIHR); Grant number: 69013 (to D.R.W.); Grant sponsor: the Natural Sciences and Engineering Research Council of Canada (NSERC); Grant numbers: 170363 and scholarships (to J.M.P.P. and D.J.G.); Grant sponsor: the Canadian Foundation for Innovation (CFI); Grant sponsor: the Canada Research Chairs Program (to D.R.W.); Grant sponsor: the Alberta Ingenuity Fund (to J.M.P.P.); Grant sponsor: Killam (to J.M.P.P.).

*CORRESPONDENCE TO: Douglas Wylie, Ph.D, Department of Psychology, University of Alberta, Edmonton, Alberta Canada T6G 2E9.
E-mail: dwylie@ualberta.ca

Received 13 May 2009; Revised 11 June 2009; Accepted 30 July 2009
DOI 10.1002/cne.22192
Published online August 7, 2009 in Wiley InterScience (www.interscience.wiley.com).

Ahn et al., 1994; Hawkes and Herrup, 1995), which is expressed by Purkinje cells. Zebrin-immunopositive (zebrin+) Purkinje cells are distributed as a parasagittal array of stripes, separated by zebrin-immunonegative (zebrin−) stripes (e.g., Larouche and Hawkes, 2006). Zebrin parasagittal stripes have been shown in several mammalian species (for review, see Sillitoe et al., 2005), and recently we have shown that zebrin is also expressed in the avian cerebellum in a similar pattern (Fig. 1C–E; Pakan et al., 2007; Iwaniuk et al., 2009). Thus, the pattern of zebrin stripes is highly conserved among species, and likely contributes to underlying fundamental cerebellar function.

The pigeon vestibulocerebellum (VbC) is an ideal system for examining the correlations among functional, anatomical, and molecular topographies of the cerebellar cortex for several reasons. First, the pigeon VbC is organized into easily identifiable zones that differ with respect to visual (i.e., optic flow) preference (Fig. 1B,CF; Wylie and Frost, 1999). Second, the climbing fiber input from the inferior olive (IO) has been extensively documented (Fig. 1F; Wylie and Frost, 1999; Crowder et al., 2000; Pakan et al., 2005), and the topography has been confirmed with single-unit recordings (Winship and Wylie, 2001). Third, the major source of optic flow MF afferents arises from two retinal recipient nuclei, the nucleus of the basal optic root (nBOR; Fig. 2A) of the accessory optic system (AOS), and the pretectal nucleus, lentiformis mesencephali (LM; Fig. 2B). The LM and nBOR have been extremely well characterized (Winterson and Brauth, 1985; Wylie and Frost, 1990; Wylie and Crowder, 2000).

Finally, in pigeons, the most striking and reliable zebrin stripes were seen in folium IXcd (Pakan et al., 2007), which, along with folium X, comprises the VbC (Figs. 1A,D,E, 2G). The lateral part of the VbC is the flocculus, which is responsive to visual stimuli resulting from rotational self-motion ADDIN EN.CITE (Wylie and Frost, 1993; Voogd and Wylie, 2004), and the medial part of the VbC consists of the ventral uvula (folium IXcd) and the nodulus (folium X), which are responsive to visual stimuli resulting from translational self-motion (Wylie and Frost, 1991; Wylie et al., 1993, 1998; Wylie and Frost, 1999). In pigeons, it has been shown that these optic flow responses are organized into parasagittal zones throughout the VbC (Fig. 1B; Wylie et al., 1993; Wylie and Frost, 1999; Winship and Wylie, 2003).

The LM is homologous to the mammalian nucleus of the optic tract; (NOT; Collewijn, 1975; Hoffmann and Schoppmann, 1975; McKenna and Wallman, 1985), and the nBOR is the homolog of the mammalian medial terminal nucleus (Simpson, 1984; Giolli et al., 2006). Neurons in the pretectum and AOS have large, contralateral receptive fields and exhibit direction selectivity in response to large-field moving visual stimuli (Burns and Wallman, 1981; Simpson, 1984; Winterson and Brauth, 1985; Simpson et al., 1988; Grasse and Cynader, 1990; Wylie and Frost, 1990). The visual MF projections to the VbC target folium IXcd but not X, and originate from large multipolar cells in the LM (mainly the lateral subnucleus) and nBOR (Fig. 2C,E,H). The LM and nBOR also project indirectly to the VbC via the medial column of the IO (mcIO), and terminate as CFs in folia IXcd and X (Clarke, 1977; Brecha et al., 1980; Gamlin and Cohen, 1988; Arends and Voogd, 1989; Lau et al., 1998; Wylie et al., 1999a; Crowder et al., 2000; Winship and Wylie, 2003). The projections to these olivocerebellar pathways originate from small fusiform cells in the intercalated (LMi) region of the LM and the dorsal regions of the nBOR (Fig. 2D,F,I; Brecha et al., 1980; Gamlin and Cohen, 1988; Wylie and Linkenhoker, 1996; Winship and Wylie, 2003; Pakan et al., 2006; Pakan and Wylie, 2006; Wylie et al., 2007).

Abbreviations

AOS	accessory optic system
Au	auricle
BDA	biotinylated dextran amine
Cb	cerebellum
CF	climbing fiber
CP	posterior commisure
CSA	complex spike activity
dl	dorsal lamella of the inferior olive
FRL	lateral mesencephalic reticular formation
FRM	medial mesencephalic reticular formation
GLv	ventral leaflet of the lateral geniculate nucleus
Hy	hypothalamus
ICo	nucleus intercollicularis
Imc	nucleus isthmi, pars magnocellularis
IO	inferior olive
IS	interstitial nucleus (of Cajal)
IXcd	folium IXcd
LM (l, m, i)	nucleus lentiformis mesencephali, (lateral, medial, intercalated)
LPC	nucleus laminaris precommisuralis
mcIO	medial column of the inferior olive
MF	mossy fiber
nBOR (d,p.l)	nucleus of the basal optic root (dorsal, proper, lateral)
NOT	nucleus of the optic tract
N-T	nasal-to-temporal
NXII	12th cranial verve (hypoglossal nerve)
PPC	nucleus principalis precommisuralis
R	raphe
rH45	rotation about the vertical axis oriented 45° from midline
Rt	nucleus rotundus
Ru	nucleus ruber (red nucleus)
rVA	rotation about the vertical axis
SOp	stratum opticum
SP	nucleus subpretectalis
TeO	optic tectum
TIO	tractus isthmo-opticus
T-N	temporal-to-nasal
TrO	tractus opticus
TT	tectothalamic tract
VbC	vestibulocerebellum
vl	ventral lamella of the inferior olive
VTA	ventral tegmental area
X	folium X
zebrin+	zebrin II-immunopositive
zebrin−	zebrin II-immunonegative

In a recent study (Pakan and Wylie, 2008), we investigated the organization of this visual olivocerebellar pathway by making small injections of anterograde tracers into the IO in order to label CF projections to the flocculus. We then correlated the resulting CF labeling with zebrin expression and found that a single parasagittal zone spans an entire zebrin+ and zebrin− stripe (Fig. 1F).

How the visual MF pathways from the LM and nBOR are organized in folium IXcd is unknown. In the present study, we made small injections of the anterograde tracer biotinylated dextran amine (BDA) into the LM and nBOR in pigeons for three reasons: 1) to determine whether there is a parasagittal organization of LM and nBOR MF terminals in folium IXcd; 2) to determine whether the LM and nBOR have differential MF projections to the VbC; and 3) to determine whether the MF pathways to folium IXcd relate to the parasagittal organization of the zebrin stripes.

MATERIALS AND METHODS

Surgical procedures

The methods reported herein conformed to the guidelines established by the Canadian Council on Animal Care and were approved by the Biosciences Animal Care and Policy Committee at the University of Alberta. Silver King and Homing pigeons (*Columba livia*), obtained from a local supplier (Vandermeer Farms, Sherwood Park, Alberta, Canada), were anesthetized by an intramuscular injection of a ketamine (65 mg/kg)/xylazine (8 mg/kg) cocktail, and supplemental doses were administered as necessary. Animals were placed in a stereotaxic device with pigeon ear bars and a beak bar adapter so that the orientation of the skull conformed to the atlas of Karten and Hodos (1967). To access the LM and nBOR, bone and dura were removed from the dorsal surface of the caudal telencephalon, lateral to the midsagittal sinus. To record the activity of optic flow units in the LM and nBOR, glass micropipettes filled with 2 M NaCl, with tip diameters of 4–5 μm, were advanced through the telencephalon and into the midbrain by using a hydraulic microdrive (Frederick Haer, Bowdoin, ME.). Stereotaxic coordinates were used to approach the LM and nBOR, but to ensure that our injections were in the desired nucleus, the localization was confirmed by recording the responses of neurons to a large (90° × 90°) moving hand-held stimulus in various areas of the visual field.

Cells responsive to optic flow stimuli were found along the track at several depths so that the injection could be placed at a depth between the most dorsally and ventrally identified cells. Once the desired area was isolated, the recording electrode was replaced with a micropipette (tip diameter 20–30 μm) containing fluorescent BDA; either mini-ruby (red; D-3312) or mini-emerald (green; D-7178; 10,000 molecular weight; Invitrogen, Carlsbad, CA). The tracers (0.01–0.05 μl of 10% solution in 0.1 M phosphate buffer) were pressure injected by using a Picospritzer II (General Valve Corporation, Fairfield, NJ). After surgery the craniotomy was filled with bone wax and the wound was sutured. Birds were given an intramuscular injection of buprenorphine (0.012 mg/kg) as an analgesic.

After a recovery period of 3–5 days, the animals were deeply anesthetized with sodium pentobarbital (100 mg/kg) and immediately transcardially perfused with phosphate-buffered saline (PBS; 0.9% NaCl, 0.1 M phosphate buffer) followed by 4% paraformaldehyde in 0.1 M PBS (pH 7.4). The brain was extracted from the skull and immersed in paraformaldehyde for 7 days at 4°C. The brain was then embedded in gelatin and cryoprotected in 30% sucrose in 0.1 M PBS overnight. Using a microtome, frozen serial sections in the coronal plane (40 μm thick) were collected throughout the rostrocaudal extent of the cerebellum.

Immunohistochemistry

Tissue sections were rinsed thoroughly in 0.1 M PBS and blocked with 10% normal donkey serum (Jackson ImmunoResearch, West Grove, PA) and 0.4% Triton X-100 in PBS for 1 hour. Tissue was then incubated in PBS containing 0.1% Triton X-100 and the primary antibody, mouse monoclonal anti-zebrin II (kindly provided by Richard Hawkes, University of Calgary; Brochu et al., 1990) for 60–75 hours at room temperature. Anti-zebrin II is a monoclonal antibody grown in mouse, produced by immunization with a crude cerebellar homogenate from the weakly electric fish *Apteronotus* (Brochu et al., 1990) and recognizes in mouse a single polypeptide band with an apparent molecular weight of 36 kDa, which cloning studies have shown to be the metabolic isoenzyme aldolase C (Ahn et al., 1994; Hawkes and Herrup, 1995). Anti-zebrin II Western blot analysis of homogenate of pigeon cerebellum also detects a single immunoreactive polypeptide band, identical in size to the band detected in extracts from the adult mouse cerebellum (Pakan et al., 2007). It was used directly from spent hybridoma culture medium diluted 1:200. Tissue was then rinsed in PBS, and sections were incubated in either Cy3 (red) or Cy2 (green) conjugated donkey anti-mouse antibody (Jackson ImmunoResearch: diluted 1:100 in PBS, 2.5% normal donkey serum, and 0.4% Triton X-100) for 2 hours at room temperature. The tissue was then rinsed in PBS and mounted onto gelatinized slides for viewing.

Microscopy and image analysis

Sections were viewed with a compound light microscope (Leica DMRE) equipped with the appropriate fluorescence filters (rhodamine and fluorescein isothiocyanate [FITC]). Images were acquired by using a Retiga EXi

FAST Cooled mono 12-bit camera (Qimaging, Burnaby BC) and analyzed with OPENLAB imaging software (Improvision, Lexington MA). Adobe Photoshop (Adobe Systems, San Jose, CA) was used to compensate for brightness and contrast.

Nomenclature

As in mammals, the cerebellum in birds is highly foliated, but is restricted to a vermis without hemispheres. Folia IXcd (uvula) and X (nodulus) comprise the VbC and merge rostrolaterally to form the auricle (Figs. 1A,B, 2G). We use the term *auricle* as a gross anatomical term and it is included in the flocculus as its lateral portion. Larsell (1967) considered the lateral extensions of folium IXcd and X as the paraflocculus and flocculus, respectively. In recent years we (Wylie and Frost, 1999; Winship and Wylie, 2003; Wylie et al., 2003a,b) divided the VbC into flocculus, nodulus, and ventral uvula based on function and homology with mammals. Purkinje cells throughout the VbC respond to optokinetic stimulation (e.g., Wylie et al., 1993). In the medial half, the complex spike activity (CSA) of Purkinje cells responds best to patterns of optic flow resulting from self-translation (Wylie et al., 1993, 1998). In the lateral half of the IXcd and X, CSA responds best to optic flow resulting from self-rotation about the vertical axis (rVA neurons; zones 0 and 2; Fig. 1B) or a horizontal axis oriented 45° contralateral azimuth/135° ipsilateral azimuth to the midline (referred to as rH45 neurons for simplicity; zones 1 and 3; Fig. 1B; Wylie and Frost, 1993).

These responses are essentially identical to those observed in the mammalian flocculus (Graf et al., 1988; Wylie and Frost, 1993). Thus, we consider these zones in the lateral half of both IXcd and X, including the auricle, as the flocculus. In mammals, a similar phenomenon has occurred: parts of the cerebellum traditionally included in the ventral paraflocculus are now considered part of the "floccular region," "lobe," or "complex" (Voogd and Barmack, 2006). The numbering of the floccular zones, 0–3 as shown in Figure 1, follows that used for rats and rabbits (Voogd and Wylie, 2004).

In folium IXcd, it is usually impossible to tell on a coronal section precisely where the border is between the uvula and the flocculus, as this division can usually only be established by electrophysiological means; however, with the correlation of zebrin immunostaining and CF borders, we (Pakan and Wylie, 2008) have determined that the medial border of the flocculus consistently corresponds to the medial edge of P4+. In what follows, we have used this guideline to determine the mediolateral boundaries of the uvula and flocculus in folium IXcd.

For the nomenclature of the LM, we relied on Gamlin and Cohen (1988), who divided the LM into a medial and a lateral subdivision (LMm and LMl, respectively; Fig. 2). Both subnuclei contain large multipolar cells, which project to the VbC (Fig. 2E; Gottlieb and McKenna, 1986; Gamlin and Cohen, 1988; Pakan et al., 2006). A strip of smaller fusiform cells was located caudally along the border of the LMm and LMl projecting to the IO. We refer to this region as the LMi (Fig. 2F; Pakan et al., 2006).

Brecha et al. (1980) divided the nBOR complex into three regions, the proper (nBORp), dorsal (nBORd), and lateral (nBORl). The large multipolar cells projecting to the VbC are found in the nBORp and nBORl (Fig. 2C). The IO-projecting cells are found in the dorsal regions of the nBORp and in the nBORd (Fig. 2D; Wylie et al., 2007, 2001).

RESULTS

Injection sites and inferior olive labeling

The results are based on 12 injections in eight animals. Four animals received single injections of red-BDA, two in the LM (Cases #2 and #8) and two in the nBOR (Cases #4 and #1). The remaining animals received injections in both the LM and the ipsilateral nBOR (Cases #6, #3, #5, and #7). Representative injection sites are shown in Figure 4A and B from Case #6 as well as in Figure 6B and 7B from Case #5. All injections were largely confined to the target region, with the exception of the LM injection in Case #7, which spread ventrolaterally into the optic tectum, and

Figure 1. Parasagittal organization of the pigeon flocculus. **A:** Photograph of the posterior pigeon cerebellum, indicating the vestibulocerebellum (VbC; folia IXcd and X), as well as their lateral extension forming the auricle (Au). **B:** Purkinje cell response properties in folium IXcd. The flocculus, the lateral portion, responds best to rotational optic flow about either the vertical axis (rVA; green) or an horizontal axis oriented 45° to midline (rH45; blue; Graf et al., 1988; Wylie and Frost, 1993). Zones in the medial part of the ventral uvula and nodulus (teal, orange, and yellow), responds best to translational optic flow stimuli (see Wylie and Frost, 1999). **C:** Photomicrograph of zebrin expression in the pigeon cerebellum, illustrating subsets of Purkinje cells that are immunopositive for zebrin (ZII+) separated by subsets of Purkinje cells that are immuonegative (ZII−). **D,E:** Pattern of zebrin II expression in the pigeon posterior cerebellum (adapted from Pakan et al., 2007), shown with a coronal section through the posterior cerebellum (D) and a schematic of the pattern of zebrin II-positive stripes (E). The zebrin stripes are numbered from 1 to 7 through folium IXcd. **F:** The rVA and rH45 cells are organized into four zones in the flocculus: two rVA zones (0 and 2, green) interdigitated with two rH45 zones (1 and 3, blue). The rVA and rH45 zones receive climbing fiber input from the caudal and rostral medial column of the inferior olive (mcIO), respectively. The caudal mcIO projects to the P4+/− (zone 0) and the P6+/− zebrin stripes (zone 2) and the rostral mcIO projects to the P5+/− (zone 1) and the P7+/− zebrin stripes (zone 3). dl, vl, dorsal and ventral lamellae of the inferior olive; gl, granular layer; ml, molecular layer; pcl, Purkinje cell layer. A magenta-green copy of this figure is available as Supplementary Figure S1. Scale bar equals; 1 mm in A,D,E (that in E also applies to B); 100 μm in C.

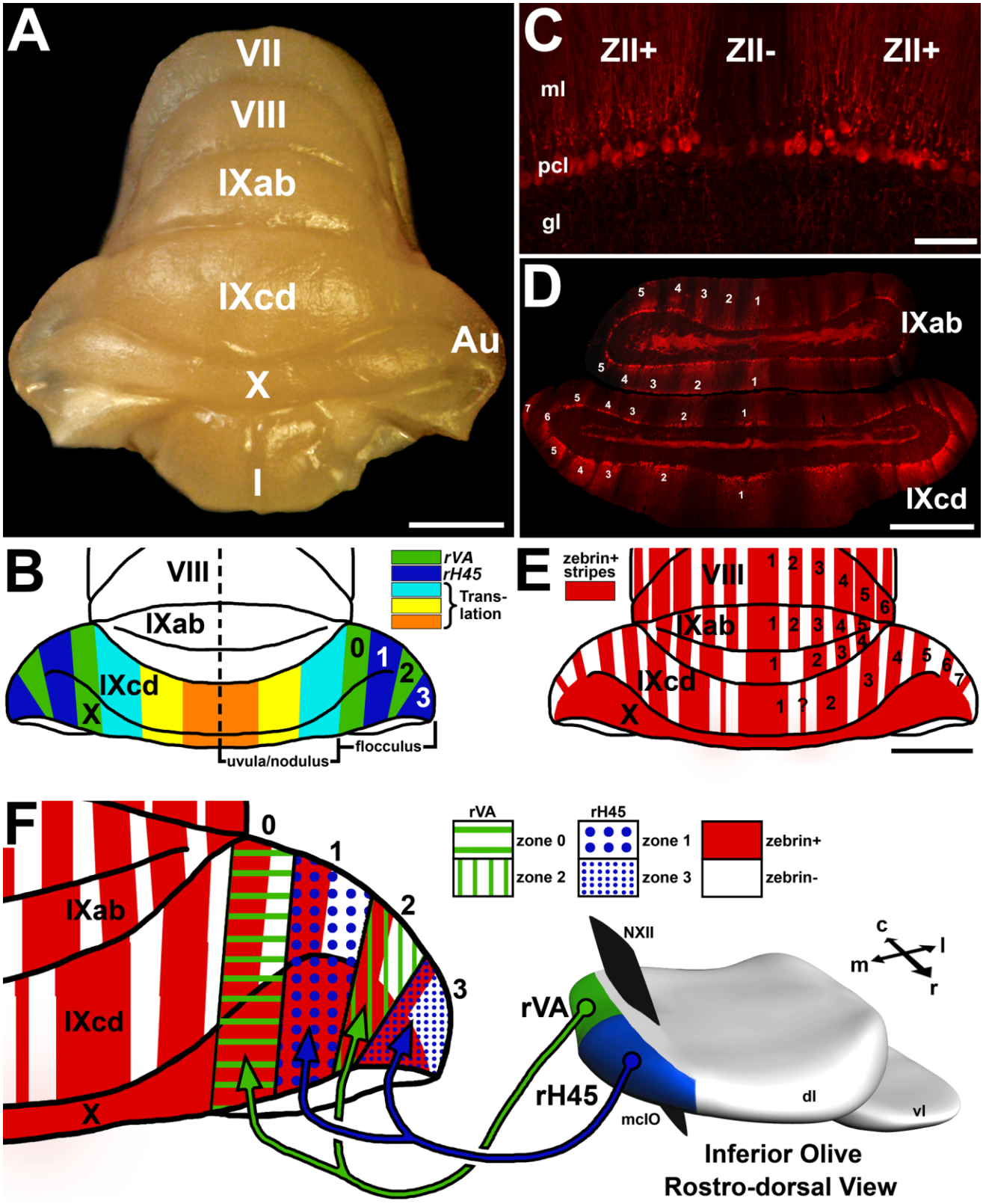
A
VII
VIII
IXab
IXcd
Au
X
I
C
ZII+
ZII-
ZII+
ml
pcl
gl
D
IXab
IXcd
B
VIII
IXab
IXcd
X
rVA
rH45
Trans-
lation
0
1
2
3
uvula/nodulus
flocculus
E
zebrin+
stripes
VIII
IXab
IXcd
X
F
IXab
IXcd
X
0
1
2
3
rVA
zone 0
zone 2
rH45
zone 1
zone 3
zebrin+
zebrin-
NXII
rVA
rH45
mclO
dl
vl
c
l
m
r
Inferior Olive
Rostro-dorsal View

Figure 1

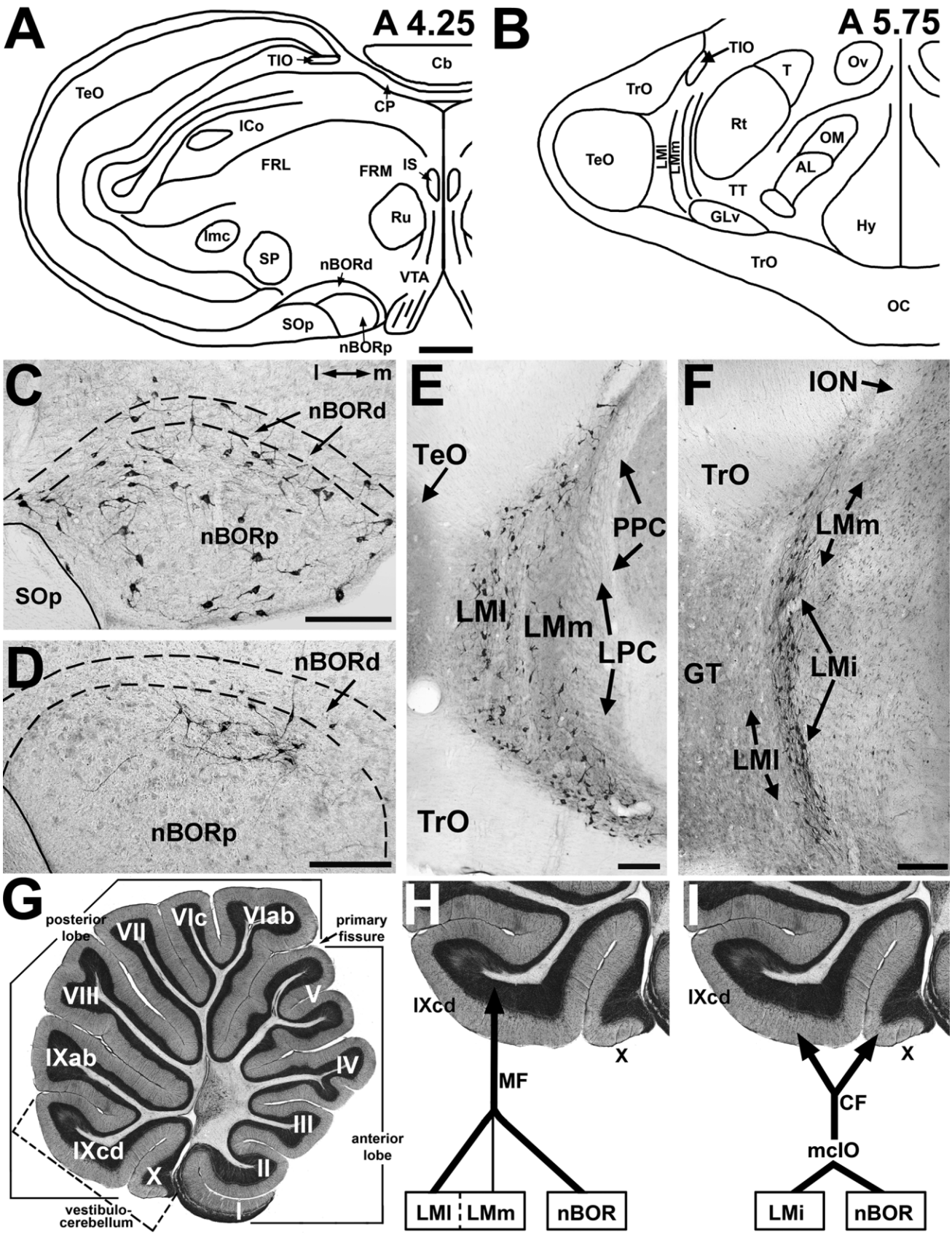
A
A 4.25
TIO
Cb
TeO
CP
ICo
FRL
FRM
IS
Ru
Imc
SP
nBORd
VTA
SOp
nBORp
B
A 5.75
TIO
Ov
T
TrO
Rt
OM
TeO
LMl
LMm
AL
TT
GLv
Hy
TrO
OC
C
l
m
nBORd
nBORp
SOp
D
nBORd
nBORp
E
TeO
PPC
LMl
LMm
LPC
TrO
F
ION
TrO
LMm
GT
LMi
LMl
G
posterior lobe
VII
VIc
VIab
primary fissure
VIII
V
IXab
IV
III
IXcd
X
II
I
anterior lobe
vestibulo-cerebellum
H
IXcd
X
MF
LMl
LMm
nBOR
I
IXcd
X
CF
mclO
LMi
nBOR

Figure 2

Case #3, which spread dorsally and slightly medially to nBOR. Because there are no mossy fiber projections from these regions of spread to the cerebellum, this has no bearing on our results.

Terminal labeling in the inferior olive was observed from all injections. The graph in Figure 3A shows the extent of the labeling that was observed in the mcIO from each injection. From injections in the nBOR, terminal labeling in the IO was heavy, with the majority of terminals found in the rostral half of the ipsilateral mcIO (thick red bars in Fig. 3A; Fig. 3B,D,E). In these rostral regions, terminals here were heaviest in the most medial regions of the mcIO, where olivary cells respond to visual stimuli resulting from rotational self-motion (Winship and Wylie, 2001). There was also a comparatively small amount of terminal labeling more caudally in the mcIO (thin red bars in Fig. 3A), as well as in the contralateral mcIO (Fig. 3E). However, labeling in these regions tended to be more lateral in the mcIO (in regions surrounding the 12th cranial nerve), where olivary cells respond to visual stimuli resulting from translational self-motion (Fig. 3B,E; Winship and Wylie, 2001). Fibers could be seen crossing the midline ventral to the raphe nucleus (Fig. 3E). The contralateral labeling from the nBOR spanned the same rostral-caudal extent as the ipsilateral labeling (ipsilateral extent is shown in Fig. 3A). From injections in the LM, labeling was observed in the caudal half of the ipsilateral IO, where terminals were found throughout the mediolateral extent of the mcIO (Fig. 3B,C). No labeling from LM injections was found in the contralateral mcIO or more rostral regions. Comparatively, the terminal labeling observed in the IO was much heavier from injections in the nBOR than from LM injections.

Figure 2. Nomenclature of the pigeon nucleus of the basal optic root (nBOR), lentiformis mesencephali (LM), and vestibulocerebellum (VbC). **A,B:** Tracings of coronal sections through nBOR and LM, respectively. The approximate anterior-posterior locations according to the atlas of Karten and Hodos (1967) are listed in the top right. **C,D:** Photomicrographs of coronal sections through the nucleus of the basal optic root (nBOR), showing retrogradely labeled neurons from injections of cholera toxin subunit B into the VbC (C) and inferior olive (D; adapted from Wylie et al., 2007). Cells projecting to the VbC are very large multipolar cells found throughout the nBOR (C). Cells projecting to the medial column of the inferior olive (mcIO) include a cluster of small cells dorsally in the nBOR (D). **E,F:** Photomomicrographs showing retrogradely labeled cells in the nucleus lentiformis mesencephali (LM) after injections of cholera toxin subunit B in the VbC (E) or inferior olive (F; adapted from Pakan et al., 2006). The cells projecting to the VbC are large multipolar cells found throughout the LM, but mainly in the lateral subnucleus (LMl), whereas those projecting to the inferior olive are localized to a strip caudally, along the border of the LMm and LMl, in the LM intercalated (LMi). **G:** Photomicrograph of a sagittal section through the pigeon cerebellum. The folia are numbered I–X (anterior to posterior) according to the nomenclature of Larsell (1967). The VbC includes folia IXcd and X. **H:** The granular layer of folium IXcd of the VbC receives direct mossy fiber projections from the LM and nBOR. The LM and nBOR also project indirectly to the VbC via the inferior olive, which then sends climbing fibers to the molecular layer of folia IXcd and X. For abbreviations see list. Scale bars equals; 1 mm in A (applies to A,B); 200 μm in C–F.

Mossy fiber input to folium IXcd

Axons from the nBOR and LM travel from the injection sites and enter the brachium conjunctivum cerebellopetal, where they then course caudally to the cerebellum, through the cerebellar white matter, and enter the granule cell layer as discrete fascicles organized in parasagittal bands (e.g., Fig. 4E). These fascicles pass through the internal regions of the granule cell layer and then spread horizontally to terminate as MFs, generally, in the external half of the granule cell layer, directly subjacent to the Purkinje cells (e.g., Fig. 4C,D). From all injections, MF terminal labeling (MF rosettes) could clearly be seen in the granule cell layer in folium IXcd of the VbC (e.g., Figs. 4, 5).

As a representation of a typical double injection case, Figures 6–8 show photomicrographs of injection sites from Case #5 (Figs. 6B, 7B) as well as the resulting MF terminal labeling in the form of reconstructions through the rostrocaudal extent of the dorsal and ventral lamellae of folium IXcd. The general pattern of terminal labeling was consistent between cases, although the total number of MF rosettes differed according to the size of the injection. For quantification, MF rosettes were counted from serial coronal sections, and the numbers that follow are percentages averaged over all cases (Table 1).

Mossy fiber projections from nBOR

By examining the MF terminal organization in Figure 6C and Table 1, the following observations can be made. MF projections from the nBOR were distributed bilaterally throughout folia IXcd in parasagittal clusters of varying widths, with slightly heavier MF labeling on the contralateral side (ipsilateral labeling 45.6%, contralateral labeling 54.4%). More terminal labeling was seen in caudal regions of the folium, and labeling in rostral regions was sparse. There was also heavier terminal labeling in the dorsal lamella (55.6%) compared with the ventral lamella (44.4%), especially on the contralateral side and in rostral regions where the ventral lamella was nearly void of terminals (e.g., Fig. 8B). With respect to the parasagittal organization, the heaviest cluster of terminal labeling occurred surrounding the midline (20.5% directly surrounding midline, bilaterally), with the exception of the ipsilateral dorsal lamella, which had very few MF terminals (ipsilateral dorsal lamella 1.1%, compared with contralateral dorsal lamella 6.4%; see green MFs in Fig. 8B for example). There were more apparent MF parasagittal clusters on the ipsilateral side, especially in the ventral lamella, where a total of five clusters

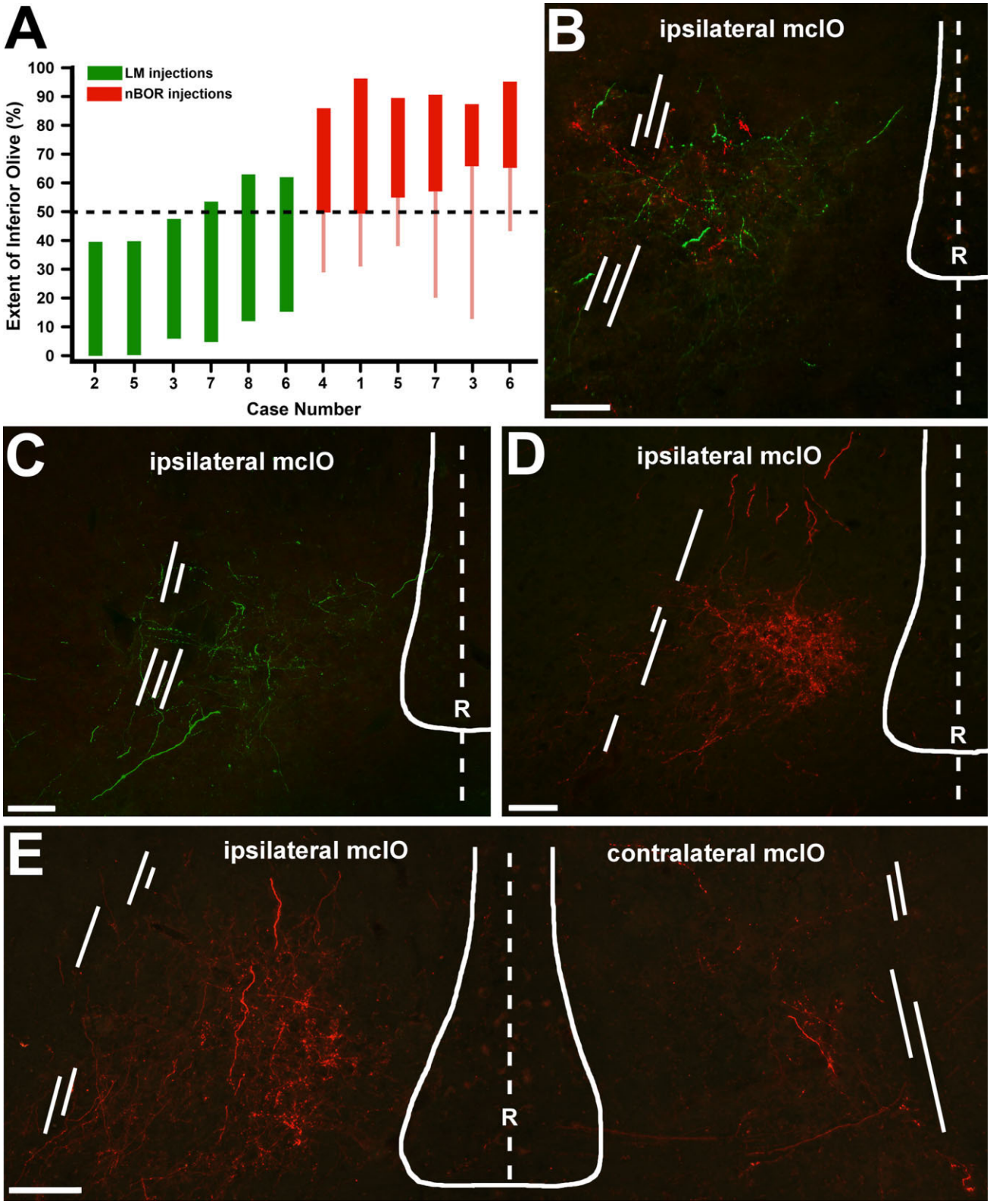
A
LM injections
nBOR injections
Extent of Inferior Olive (%)
100
90
80
70
60
50
40
30
20
10
0
2 5 3 7 8 6 4 1 5 7 3 6
Case Number
B
ipsilateral mcIO
R
C
ipsilateral mcIO
R
D
ipsilateral mcIO
R
E
ipsilateral mcIO
contralateral mcIO
R

Figure 3

could be distinguished. In the dorsal lamella, there was a heavier MF projection to the uvula compared with the flocculus. The pattern of MF labeling in the dorsal flocculus was similar to that in the ventral flocculus, with a total of three main parasagittal bands throughout its rostrocaudal extent. There was generally one parasagittal zone in the most lateral regions of the dorsal flocculus that received a small number of mossy fiber projections; this zone was seen consistently on the ipsilateral side and in the cases with large injections sites, few MF terminals were seen in the corresponding region on the contralateral side.

Mossy fiber projections from LM

The organization of MF projections from the LM was similar to the distribution seen from nBOR injections, and MF terminals were generally in overlapping regions (e.g., Figs. 5A,B, 8A–C). By examining the MF terminal organization in Figure 7C and Table 1, the following observations can be made. From LM injections, MFs were distributed bilaterally, and terminal labeling was heavier on the contralateral side (ipsilateral labeling 35.3%, contralateral labeling 64.7%). More terminal labeling was seen in caudal regions of the folium. Heavier MF terminal labeling was seen in the dorsal lamella (60.7%) compared with the ventral lamella (39.3%), especially in contralateral and rostral regions. With respect to the parasagittal organization, clusters were more apparent from the LM injections compared with nBOR injections. As with the nBOR, LM injections also heavily labeled the midline region, with the exception of the ipsilateral dorsal lamella (see Fig. 8B for example); this pattern was more pronounced from injections in the LM (ipsilateral dorsal lamella 1.2%, compared with contralateral dorsal lamella 13.7%).

In the ventral lamella, there were more apparent parasagittal clusters on the ipsilateral side, where four clusters could be distinguished. In the dorsal lamella, there was a heavier MF projection to the uvula compared witho the flocculus, and overall, the heaviest labeling was observed in the contralateral dorsal uvula. The pattern of MF terminals in the flocculus consisted of three main parasagittal bands throughout its rostrocaudal extent. From LM injections, there was also generally one parasagittal zone in the most lateral and dorsal flocculus, with more rosettes on the ipsilateral compared with the contralateral side (Fig. 5C).

Comparison of projections from LM and nBOR

Because the labeling from the LM and nBOR was by and large overlapping, the parasagittal bands are more obvious in Figure 8C. There were a few notable differences between LM and nBOR injections in the pattern of MF labeling. Figure 8C shows the reconstruction of the labeling from both the LM and the nBOR. The MF terminal labeling in the flocculus was similar from LM and nBOR injections, but, on average, the MF terminal labeling in the uvula was more horizontally dispersed from the nBOR compared with the LM.

Projections outside folium IXcd

The projections from the LM and nBOR to other regions of the cerebellum were not the focus of the current study, but briefly, from injections in nBOR, we observed very few MF terminals in other folia of the posterior lobe (folia VI–IXab), and most of the terminals were found surrounding the midline of these folia. From injections in the LM, substantially more MF terminals were observed in the posterior lobe, especially in folia VI–VIII, and the terminals were found in the highest density surrounding the midline, with additional clusters in the more lateral parts of the folia. From injections into the LM and nBOR we also observed a small number of MF terminals in the lingula (folium I) in the anterior lobe. No mossy fiber terminals were observed in folium X of the VbC in any of the cases.

Zebrin expression in folium IXcd

Zebrin immunoreactivity is observed in the Purkinje cell dendritic arbors, somata, and axons, but not the nuclei (Fig. 1C). In the pigeon posterior lobe, clusters of strongly

Figure 3. Pattern of terminal labeling in the inferior olive from injections in the nucleus lentiformis mesencephali (LM) and the nucleus of the basal optic root (nBOR). **A:** Graph of the rostrocaudal extent of terminal labeling observed in the medial column of the inferior olive (mcIO) resulting from injections of anterograde tracers into the nucleus lentiformis mesencephali (LM; green bars) and the nucleus of the basal optic root (nBOR; red bars). The bars represent the presence of terminal labeling in the mcIO in the corresponding rostrocaudal region of the inferior olive, normalized and averaged over all cases. Thin red bars represent a comparatively small amount of labeling more caudal in the mcIO from nBOR injections. **B:** Photomicrograph of terminal labeling in the ipsilateral caudal mcIO from a green injection in LM and a red injection in nBOR. Note that the amount of terminal labeling from nBOR is small and is located laterally in the mcIO. **C:** Photomicrograph of labeling from a green injection in the LM illustrating terminal labeling in the medial and lateral regions of the mcIO. There was no terminal labeling observed in the contralateral mcIO from injections in LM. **D,E:** Photomicrographs of terminal labeling in the rostral mcIO from a red injection in the nBOR; note the heavy terminal labeling in the medial portions of the mcIO (D and E, left) and the presence of a small amount of terminal labeling in the contralateral mcIO in E (right), located slightly lateral compared with the ipsilateral labeling. E also shows fibers crossing the midline ventral to the raphe nucleus (R). Dotted lines represent midline; broken lines represent the position of the 12th cranial nerve, which is used as a landmark for the lateral edge of the mcIO. A magenta-green copy of this figure is available as Supplementary Figure S2. Scale bar equals; 100 μm in B–E.

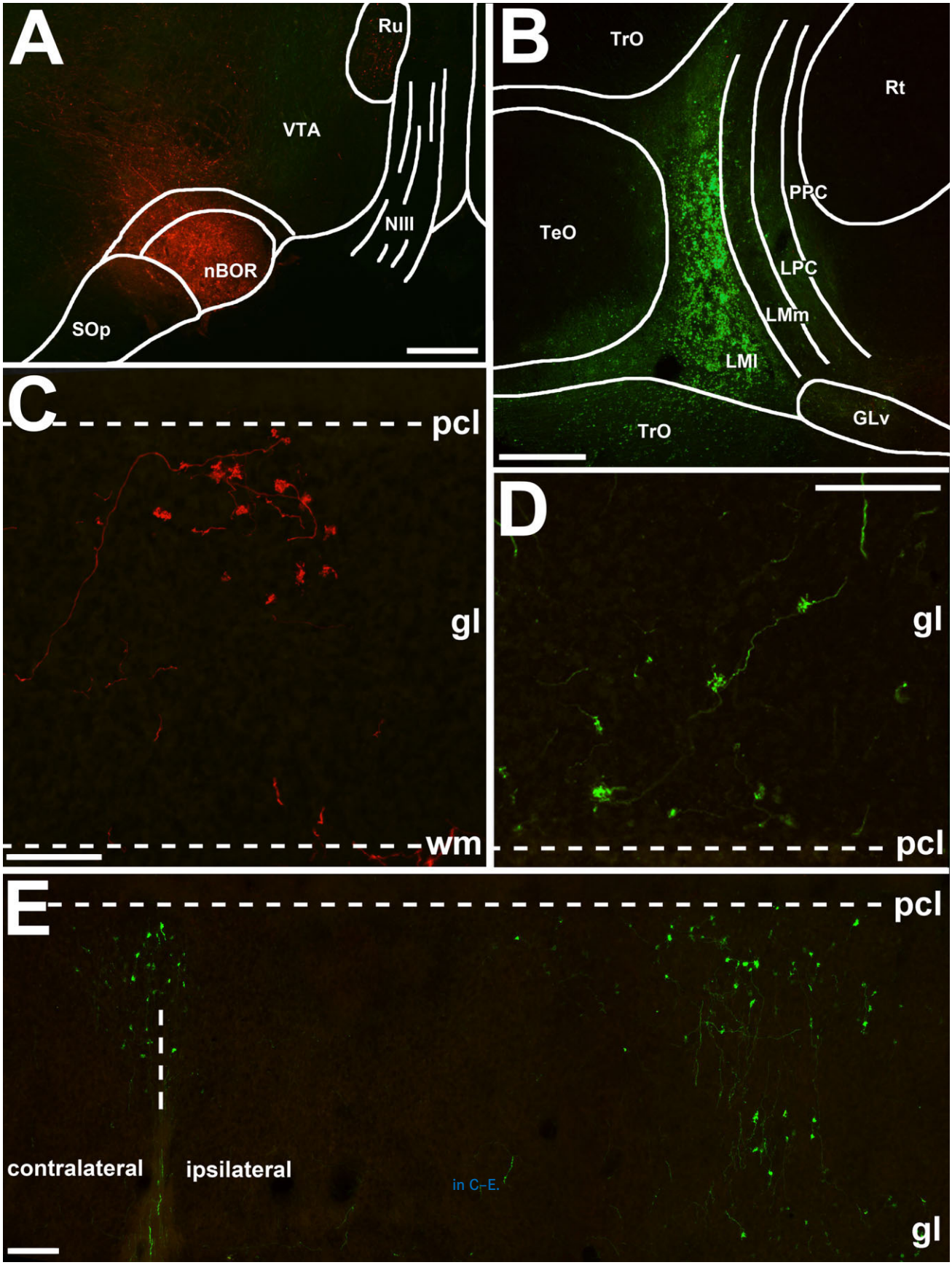
A
Ru
VTA
NIII
nBOR
SOp
B
TrO
Rt
PPC
TeO
LPC
LMm
LMl
TrO
GLv
C
pcl
gl
wm
D
gl
pcl
E
pcl
contralateral
ipsilateral
in C–E.
gl

Figure 4

zebrin-immunoreactive Purkinje cells alternate with clusters that are immunonegative or very weakly immunoreactive (Fig. 1D,E; Pakan et al., 2007). Alternating zebrin+/− stripes observed in folium IXcd are the most consistent and clear stripes seen throughout the cerebellum. The stripes themselves are numbered following the nomenclature used in Pakan et al. (2007), which is the same as that in mammals (Brochu et al., 1990; Eisenman and Hawkes, 1993; Ozol et al., 1999; Sillitoe and Hawkes, 2002; reviewed in Sillitoe et al., 2005), whereby the most medial positive stripe straddles the midline and is designated P1+ and the six other zebrin+ stripes, P2+–P7+, are located laterally on either side of the cerebellar midline extending into the auricle.

There are a few additional classifications that we have used in the current study to further delineate the various zebrin-immunoreactive boundaries. In pigeons, there is often an additional, very small (perhaps one to three Purkinje cells wide), unclassified zebrin stripe thatis between the large P1+ and P2+ stripes. We previously labeled this zone "?" in Pakan et al. (2007), because it was relatively inconsistently and usually only weakly immunopositive compared with the other surrounding positive stripes. However, in the current study, this small stripe was seen in all our cases (see Fig. 5D for example), especially in more caudal regions of folium IXcd; therefore we refer to P1-medial and P1-lateral as the zebrin-negative regions surrounding the "?" zebrin+ zone. Secondly, the P2+ zebrin stripe is quite large and has a paucity of Purkinje cells in its midregion, spanning about two to four Purkinje cells wide. Although this creates a pseudo-border, it is not a zebrin− stripe, and we refer to the portion medial to this division as P2+medial and the lateral portion as P2+lateral (see Fig. 5E for example).

Mossy fiber labeling and zebrin expression in folium IXcd

In panel D of Figures 6–8, which show the reconstructions of MF terminal labeling from the LM and nBOR as well as the zebrin expression pattern, the correlation between the MF clusters and the zebrin stripes can be directly assessed. As is evident from these representative reconstructions, we found that, generally, MF terminals from the LM and nBOR clustered within zebrin+ stripes. This can also be seen in Table 1, which shows percentages of MF terminal labeling in the various zebrin stripes, averaged across all cases.

From nBOR injections, the concordance of the MF and the zebrin+ stripes is especially apparent in the ventral lamella, where 84% of the MF terminals were in zebrin+ zones. In the dorsal lamella 76% of terminals were in zebrin+ zones. Even within the P1− zebrin zone, much of the labeling fell within the very thin band of zebrin+ Purkinje cells, referred to as the "?" zebrin+ zone. From this perspective it seems that the nBOR MF projection is organized into several bands, each associated with a zebrin+ stripe.

From the LM injections—similar to that observed in nBOR—the concordance of the MF and the zebrin+ stripes is especially apparent in the ventral lamella, where 96% of the MF terminals were in zebrin+ zones. There were some general differences in the organization of zebrin stripes and MF terminals from injections in the LM compared with the nBOR. For instance, we did not observe a main cluster of MF rosettes in the "?" parasagittal stripe from injections in the LM. Also, the parasagittal cluster corresponding to P3+ showed a striking difference between the contralateral and ipsilateral sides, with more MF terminal labeling on the contralateral side (7.3% on the contralateral compared with 1.3% on the ipsilateral side). There was also heavier terminal labeling in P4+ on the contralateral side (6.7% contralateral compared with 2.1% ipsilateral), especially in the dorsal lamella (4.0% in contralateral dorsal lamella, 0.9% in ipsilateral dorsal lamella). As is apparent from Figure 6D (and Table 1) there was very little MF terminal labeling in the zebrin− zones from LM injections. On average, through the entire rostrocaudal extent of folium IXcd, 13 of the 16 zebrin− zones had less than 1% of MF terminal labeling associated with each of them.

Although the abrupt zebrin+/− boundaries were not always strictly limiting boundaries for the MF clusters, generally, the zebrin+ Purkinje cells were directly superficial to the MF terminals. This is not an artifact of there simply being more zebrin-ositive Purkinje cells in folium IXcd. From our own measurements, we found that 57% of the Purkinje cells express zebrin (zebrin+ Purkinje cells) and 43% do not (zebrin− Purkinje cells). When we consider this along with the fact that 91% of MF terminals from LM injections and 80% of MF terminals from nBOR injections were correlated with zebrin+ stripes, it is clear that there was a strong bias for MF rosettes to cluster in zebrin+ stripes.

Figure 4. Typical injection sites in the nucleus lentiformis mesencephali (LM) and the nucleus of the basal optic root (nBOR) and the resulting pattern of mossy fiber (MF) labeling in folium IXcd. **A,B:** Photomicrographs of typical injection sites in the nBOR (A; red) and LM (B; green). C–E: Photomicrographs of typical resulting MF terminals (rosettes) in folium IXcd from injections in the nBOR (red) and LM (green). **C,D:** Note the proximity of the MF terminals in the superficial granular cell layer (gl), directly adjacent to the Purkinje cell layer (pcl) in both the dorsal lamella (C) and the ventral lamella (D). **E:** It can be seen that the MF terminal pattern is organized in parasagittally oriented clusters in the granular layer. For abbreviations see list. A magenta-green copy of this figure is available as Supplementary Figure S3. Scale bar equals; 500 μm in A,B; 100 μm in C–E.

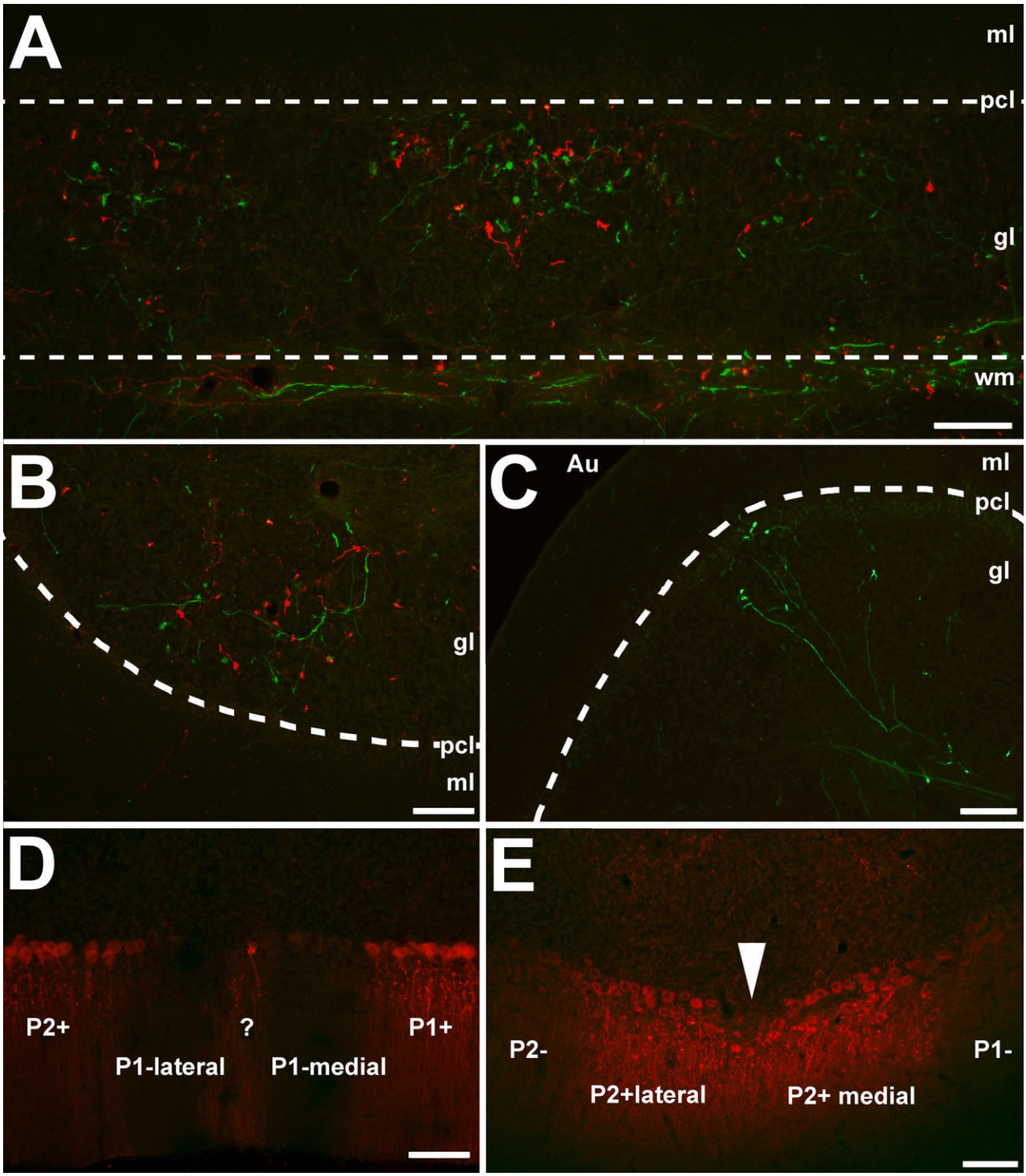

Figure 5. Pattern of mossy fiber (MF) labeling in folium IXcd from injections in the nucleus lentiformis mesencephali (LM) and the nucleus of the basal optic root (nBOR), and zebrin expression in folium IXcd. A–C: Photomicrographs of the typical pattern of resulting MF terminals (rosettes) in folium IXcd from injections in the nBOR (red) and LM (green). **A:** Example of parasagittal clusters of labeled MF terminals in the dorsal lamella. **B:** Example of parasagittal clusters of labeled MF terminals in the ventral flocculus from injections in the nBOR (red) and LM (green). **C:** Single parasagittal zone in the dorsal portions of the lateral flocculus (anatomically known as the auricle [Au]) from an injection in LM. D,E: Examples of zebrin expression in folium IXcd shown in red. **D:** The "?" zebrin-immunopositive zone, dividing the P1− zone into medial and lateral regions. **E:** Natural paucity of Purkinje cells (arrowhead) in the midregion of the P2+ zebrin-immunopositive zone, dividing the P2+ zone into medial and lateral regions. Dotted lines represent the boundaries of the granular cell layer. gl, granular layer; ml, molecular layer; Pcl, Purkinje cell layer; wm, cerebellar white matter. A magenta-green copy of this figure is available as Supplementary Figure S4. Scale bar equals; 100 μm in A–E.

DISCUSSION

The parasagittal, zonal organization of climbing fiber projections from the IO has been well established in many cerebellar systems and in many different species (Voogd et al., 2003; Sugihara et al., 2004; Sugihara and Shinoda, 2004; Voogd and Ruigrok, 2004; Pijpers et al., 2005, 2006; Schonewille et al., 2006; Sugihara, 2006). The parasagittal organization of MF projections to the cerebellum has been less thoroughly studied, but the majority of research in mammals has found a zonal arrangement of terminals (for review, see Ozol and Hawkes, 1997).

In the present study, by injecting anterograde tracers into two retinal recipient nuclei in the pretectum and AOS, we have shown that these visual MF projections terminate in a zonal organization; this resulted in a number of parasagittal clusters of MF rosettes in the superficial granular layer of folium IXcd in the pigeon VbC. Generally the pattern of MF terminal labeling was very similar between LM and nBOR injections (Fig. 8), and consisted of three to four parasagittal clusters spanning the uvula and four clusters spanning the flocculus. The parasagittal demarcations were more defined in the ventral lamella of folium IXcd, especially compared with the dorsal uvula, which showed more horizontal spread of MF terminal labeling from both LM and nBOR injections. Moreover, we showed that there was a clear organization of the MF terminals in relation to the zebrin stripes, to the extent that the bulk (80–91%) of the terminal labeling was contained within the zebrin stripes. We will consider these findings in light of what is known with regard to the visual information carried from the LM and nBOR to the VbC through the MF and olivocerebellar pathways, and the functional organization of the olivocerebellar pathways with the zebrin stripes.

Visual mossy fiber projections to the vestibulocerebellum

Previous investigations into the organization of MF terminals in the pigeon VbC using anterograde tracer (^{3}H-labeled amino acids) injections in the LM (Clarke, 1977) and nBOR (Brecha et al., 1980) have described the resulting labeling in folium IXcd as "patchy" or "varied," but the specific pattern of terminal labeling was not described. Gamlin and Cohen (1988) also used audioradiographic techniques to investigate the efferent projections from the pigeon LM, including MF pathways to the cerebellum. Similar to the current study, they found MF terminals bilaterally in folium IXcd, but more on the contralateral side, and in the external half of the granule cell layer. They did not provide a description of the organization of MF terminals, but from the samples of data provided in their figures (Figs. 1 and 5 of Gamlin and Cohen, 1988), it is clear that the MF terminals are arranged in zonal clusters, although it is impossible to interpret the specific pattern from these examples. Schwartz and Schwartz (1983) investigated the organization of primary vestibular MF terminals in the pigeon VbC. They found that the labeled MF terminals were concentrated superficially in the granule cell layer (directly adjacent to the Purkinje cell layer) but did not note a parasagittal zonal arrangement.

The direct MF pathways from the LM and nBOR to the VbC are not found in all vertebrates. Similar to pigeons, these direct MF pathways have been reported in turtles and fish, but not frogs (fish: Finger and Karten, 1978; turtle: Reiner and Karten, 1978; frogs: Montgomery et al., 1981; Weber et al., 2003). In mammals, there has been no report of a mossy fiber pathway from the NOT to the cerebellum; however, a mossy fiber projection from the medial terminal nuclei to the VbC has been reported in some species (chinchilla: Winfield et al., 1978; tree shrew: Haines and Sowa, 1985), but not others (cats: Kawasaki and Sato, 1980; rats and rabbits: Giolli et al., 1984). There is evidence of several indirect MF pathways from the NOT and the AOS to the cerebellum through which optic flow information can be conveyed. Most of the mossy fiber input to the vestibulocerebellum arises in the vestibular nuclei and the prepositus hypoglossi (Voogd et al., 1996; Ruigrok, 2003), but there are also projections originating in the reticular formation, the raphe nuclei, a number of pontine regions, and neurons located within and around the medial longitudinal fasciculus (Blanks et al., 1983; Sato et al., 1983; Gerrits et al., 1984; Langer et al., 1985; Mustari et al., 1994; Voogd et al., 1996; Nagao et al., 1997; Ruigrok, 2003). The NOT and AOS project to many of these structures, including the vestibular nuclei, the medial and dorsolateral nuclei of the basilar pontine complex, the mesencephalic reticular formation, the prepositus hypoglossi, and the nucleus reticularis tegmenti pontis (NRTP; Itoh, 1977; Terasawa et al., 1979; Cazin et al., 1982; Holstege and Collewijn, 1982; Giolli et al., 1984, 1985, 1988; Torigoe et al., 1986a,b; for review, see Simpson et al., 1988; Gamlin, 2006; Giolli et al., 2006). Serapide and colleagues (2001, 2002) have observed that MF projections from the NRTP and the basal pontine nuclei terminate in parasagittal zones in the vermis of lobule IX, the flocculus, and the paraflocculus.

Visual olivo-vestibulocerebellar pathways

In this study, we also describe the topography of projections from the LM and nBOR to the mcIO. We found a bilateral projection from the nBOR, which was much heavier to the ipsilateral mcIO, and a unilateral projection from the LM to the ipsilateral mcIO. This is in agreement with previous anterograde studies (Clarke, 1977; Brecha et al., 1980; Gamlin and Cohen, 1988; Wylie et al., 1997). We also observed a rostrocaudal difference, with the nBOR projecting heavily to the rostral regions, and the LM pro-

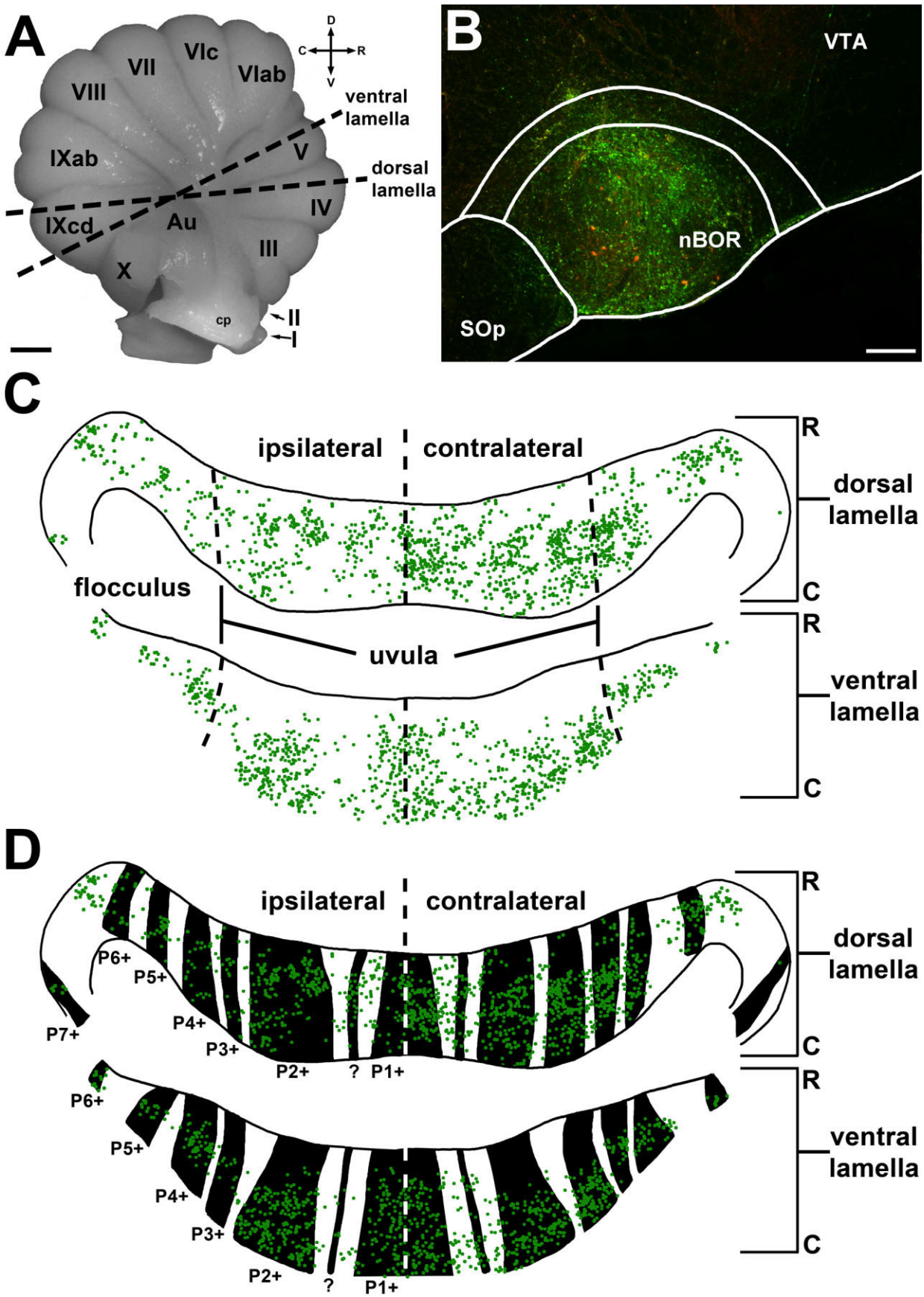
A
VII
VIc
VIab
VIII
ventral lamella
IXab
V
dorsal lamella
IV
IXcd
Au
III
X
cp
II
I
D
C
R
B
VTA
nBOR
SOp
C
ipsilateral
contralateral
R
dorsal lamella
C
flocculus
uvula
R
ventral lamella
C
D
ipsilateral
contralateral
R
dorsal lamella
C
P6+
P5+
P4+
P7+
P3+
P2+
?
P1+
R
ventral lamella
C
P6+
P5+
P4+
P3+
P2+
?
P1+

Figure 6

jecting exclusively to the caudal regions of the mcIO. This confirms the results from a retrograde study that noted more labeling of neurons in the nBOR and LM from injections in the rostral and caudal mcIO, respectively (Wylie, 2001). The differences in the projections from the LM and nBOR to the caudal and rostral mcIO, respectively, are similar to those seen in homologous pathways from the pretectum ad AOS to the dorsal cap of Kooy, the homolog of the mcIO in mammals (Mizuno et al., 1973; Maekawa and Takeda, 1976; Takeda and Maekawa, 1976; Holstege and Collewijn, 1982; Mustari et al., 1994).

Physiology of the visual projections to the VbC

Most LM and nBOR neurons have large receptive fields restricted to the contralateral eye, and respond best to large-field stimuli such as checkerboards, gratings, and random dot patterns moving in a particular direction. Generally speaking, the LM and nBOR are complementary with respect to direction preference. About half of LM neurons prefer temporal-to-nasal (T-N) motion. T-N neurons are rare in the nBOR, where neurons that prefer upward, downward, and nasal-to-temporal (N-T) motion are equally represented (Burns and Wallman, 1981; Morgan and Frost, 1981; Gioanni et al., 1984; Winterson and Brauth, 1985; Wylie and Frost, 1990, 1996). LM and nBOR neurons are also sensitive to speed (i.e., temporal frequency of moving gratings), and there are two response groups in both the nBOR and LM: fast cells and slow cells (Wylie and Crowder, 2000; Crowder and Wylie, 2001; Crowder et al., 2003; Winship et al., 2006). Recording from the VbC, Winship et al. (2005) showed that the olivocerebellar system receives input from only slow cells in the LM and nBOR, whereas the MF projections to the VbC arise from both slow and fast cells in the LM and nBOR (Fig. 9). In the LM, the slow cells prefer T-N motion, whereas in the nBOR the slow cells prefer upward, downward, or N-T motion, but not T-N motion (Wylie and Crowder, 2000; Crowder and Wylie, 2001). Thus, the visual information to the mcIO from the nBOR and LM differs with respect to direction preference, and it is not surprising that these projections are topographic.

The topography of these terminals in the mcIO is important in establishing the panoramic receptive fields of both the mcIO and Purkinje cells that are responsive to particular patterns of optic flow. For example, the caudal mcIO contains medially located rVA neurons, and the lateral regions of the caudal mcIO contain neurons that are responsive to visual stimuli resulting from self-translation in the backward direction. The preferred optic flowfield resulting from both of these response types consists of T-N motion in the contralateral hemifield. Therefore, as we have shown in the present study, one would expect this caudal region to receive a large portion of its input from the LM, which transmits T-N motion to the mcIO (see also Wylie et al., 1999b; Crowder et al., 2000; Winship and Wylie, 2001; Wylie, 2001).

The fast units in the nBOR and LM respond to all cardinal directions of motion, upward, downward, N-T, and T-N (Wylie and Crowder, 2000; Crowder and Wylie, 2001). As the MFs to the VbC originate from both fast and slow cells in the nBOR and LM (Winship et al., 2005), these nuclei are transmitting similar information to the VbC; this is not the case for the olivary inputs. Perhaps this is why the MF inputs from the nBOR and LM to the VbC are overlapping and not topographically separated as they are in the mcIO.

Visual inputs to IXcd in relation to zebrin stripes

In the present study, we are able to use the antigen zebrin II as a molecular marker in order to relate the various patterns of organization in the cerebellum. Although the specific function of zebrin II (or aldolase C) in the cerebellum is largely unknown (Welsh et al., 2002; Wadiche and Jahr, 2005), zebrin expression is useful for, and often used as, a positional landmark in the cerebellar cortex (Hawkes and Gravel, 1991; Hawkes, 1992; Hawkes et al., 1993; for review, see Herrup and Kuemerle, 1997; Ozol et al., 1999). We have previously (Pakan and Wylie, 2008) investigated the correlation between CF zones and the zebrin expression pattern in the flocculus by making small anterograde tracer injections into either the rostral or caudal mcIO and visualizing the resulting CF labeling with the zebrin stripes. We found that there was a strict concordance between CF organization and zebrin labeling such that a specific CF zone corresponded to a zebrin+/− pair in the flocculus (Fig. 1E). For instance, the most caudomedial CF zone, an rVA zone, spanned the P4+ and P4− zebrin stripes, the adjacent rH45 zone spanned the P5+

Figure 6. Reconstruction of mossy fiber (MF) terminals resulting from injections in the nucleus of the basal optic root (nBOR) from Case #5. Figure 7 shows a reconstruction of MF terminals resulting from an injection in the nucleus lentiformis mesencephali (LM) from the same case. Figure 8 shows the overlay of the MF terminal labeling from these two injections. **A:** Lateral view of the pigeon cerebellum illustrating the plane of the reconstruction through the rostrocaudal extent of the folium. **B:** Injection site in a photomicrograph of the nBOR. **C,D:** Reconstructions of folium IXcd through its rostrocaudal extent. Each dot on the reconstructions represents an MF terminal observed in serial coronal sections, but in order to present the overall pattern of labeling, the dorsal lamella and ventral lamella were separated and coronal sections were stacked from caudal to rostral. In other words, caudal coronal sections are represented more ventrally and rostral sections are represented more dorsally. D also shows the corresponding zebrin expression in folium IXcd. Au, auricle; R, rostral; C, caudal; D, dorsal, V, ventral; for other abbreviations see list. Scale bar equals; 1 mm in A; 200 μm in B.

TABLE 1.

Quantification of Mossy Fiber (MF) Rosettes Labeled in Folium IXcd From Anterograde Tracer Injections Into the Nucleus Lentiformis Mesencephali (LM) and the Nucleus of the Basal Optic Root (nBOR)[1]

	P1+	P1− med	?	P1− lat	P2+ med	P2+ lat	P2−	P3+	P3−	P4+	P4−	P5+	P5−	P6+	P6−	P7+	P7−	Total all	Total +
nBOR I	7.0	2.1	2.4	3.2	9.2	6.1	2.2	3.7	0.3	4.3	0.3	1.8	0.6	1.2	0.2	0.3	0.7	45.5	36.0
C	13.5	2.7	2.3	3.5	7.5	5.0	1.3	5.9	0.8	5.4	0.9	3.1	0.7	1.1	0.3	0.1	0.4	54.5	43.9
Bi	20.5	4.8	4.7	6.7	16.7	11.1	3.5	9.6	1.1	9.7	1.2	4.9	1.3	2.3	0.5	0.4	1.1	100	79.9
LM I	10.5	0.9	1.0	0.4	7.6	7.3	0.6	1.3	0.3	2.1	0.0	2.0	0.2	0.4	0.2	0.0	0.7	35.3	32.2
C	21.6	1.9	1.4	1.0	7.2	9.9	0.6	7.3	0.4	6.7	0.7	3.8	0.9	1.0	0.2	0.0	0.1	64.7	58.9
Bi	32.1	2.8	2.4	1.4	14.8	17.2	1.2	8.6	0.7	8.8	0.7	5.8	1.1	1.4	0.4	0.0	0.8	100	91.1

[1]MF rosettes corresponding to zebrin stripes (labeled P1+/− through P7+/−) on each side of the folium were counted from serial coronal sections and expressed as percentages of the total number of labeled rosettes per case. The numbers presented are averaged over all cases. I, ipsilateral; C, contralateral; Bi, bilateral.

and P5− stripes, the second rVA zone spanned the P6+ and P6− stripes, and the most rostrolateral rH45 zone spanned the P7+ and P7− zebrin stripes.

This relationship of zebrin stripes to parasagittal CF zones was contrary to findings in other species and other regions of the cerebellum where CF zones generally project to either zebrin+ stripes or zebrin− stripes, but not both (Voogd et al., 2003; Sugihara and Shinoda, 2004; Voogd and Ruigrok, 2004; Pijpers et al., 2006; Sugihara and Quy, 2007; Sugihara and Shinoda, 2007; Pakan and Wylie, 2008). For instance, in a comprehensive study of the entire cerebellum, Sugihara and Shinoda (2004) identified olivocerebellar projections to zebrin compartments by labeling climbing fibers with BDA injected into various small areas within the inferior olive in rats. They found that there was a correspondence between a given olivary region and zebrin stripes of a particular sign, either positive or negative, but not both.

In this study, to determine the relationship of visual MF projections to the zebrin pattern, we examined the organization of the MF terminals from the LM and nBOR to the granular layer and the parasagittal zebrin antigenic stripes in the Purkinje cells of folium IXcd in the pigeon. Consistent and well-demarcated zebrin antigenic stripes and parasagittal clusters of MF terminals from both the LM and nBOR were visualized simultaneously, enabling a direct comparison of the zonal relationship. We found that the MF terminations were more pronounced in regions where Purkinje cells were zebrin+. This was a strong relationship, with a clear correlation of MF parasagittal clusters and zebrin+ stripes; however, the zebrin-immunoreactive borders were not explicit boundaries for the MF terminals, and there were some MF rosettes observed in zebrin− regions as well.

There have been few studies investigating the relationship between MF terminal organization and zebrin expression; the results of these studies seem to implicate a consistent yet complicated relationship between MF zones and zebrin stripes (Gravel and Hawkes, 1990; Akintunde and Eisenman, 1994; Ji and Hawkes, 1994). However, a study by Matsushita et al. (1991) examined the topographic relationship between zebrin stripes and the distribution of spinocerebellar fibers originating from the central cervical nucleus in the rat. They found that in lobules I–V and VIII and the copula pyramidis, the labeled MF terminals were seen clustered beneath zebrin-positive bands. Similar to the results of this study, they also found that the borders of MF terminal distribution were not well delineated, and were not strictly bounded by the borders of zebrin-positive bands.

In general, the organization of the MF projections to the cerebellum appears less spatially restricted and seems more suited for carrying a wide divergence of information, not only because MF information originates from many different regions in the central nervous system, but also due to the indirect nature of the MF projection to Purkinje cells through granule cells and parallel fibers. In contrast, the CF system, originating solely in the IO, sends its projections directly to the Purkinje cell dendrites in narrow, parasagittally arranged stripes. The current study, along with our previous study on the CF correlation with zebrin (Pakan and Wylie, 2008), illustrates these differences between visual CF and MF projections from the pretectum and the AOS to the flocculus of the pigeon VbC. Along with the function of the Purkinje cells themselves, the organizational differences in these two afferent systems have been central to all major theories of cerebellar function (Marr, 1969; Albus, 1971; Ito, 1984); however, major portions of these theories remain largely unevaluated be-

Figure 7. Reconstruction of MF terminals resulting from injections in the nucleus lentiformis mesencephali (LM) from Case #5. **B:** Injection site in a photomicrograph of the LM. See Figure 6 legend for details of **A**, **C**, and **D**. A magenta-green copy of this figure is available as Supplementary Figure S5. Scale bar equals; 1 mm in A; 200 μm in B.

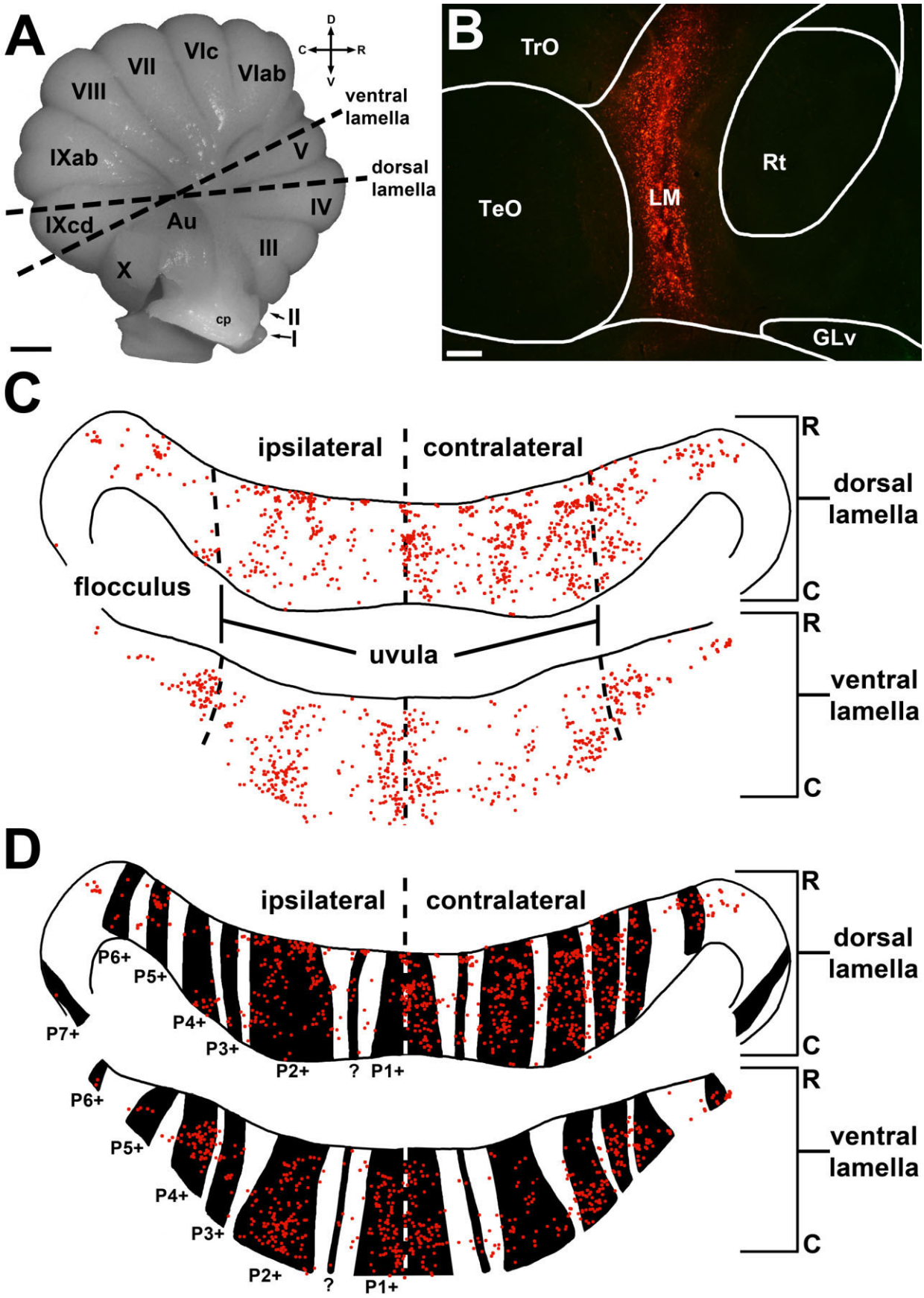
A
VII
VIc
VIab
VIII
ventral lamella
IXab
V
dorsal lamella
IV
IXcd
Au
III
X
cp
II
I
D
C
R
B
TrO
TeO
LM
Rt
GLv
C
ipsilateral
contralateral
R
dorsal lamella
C
flocculus
uvula
R
ventral lamella
C
D
ipsilateral
contralateral
R
dorsal lamella
C
P6+
P5+
P4+
P7+
P3+
P2+
?
P1+
R
ventral lamella
C
P6+
P5+
P4+
P3+
P2+
?
P1+

Figure 7

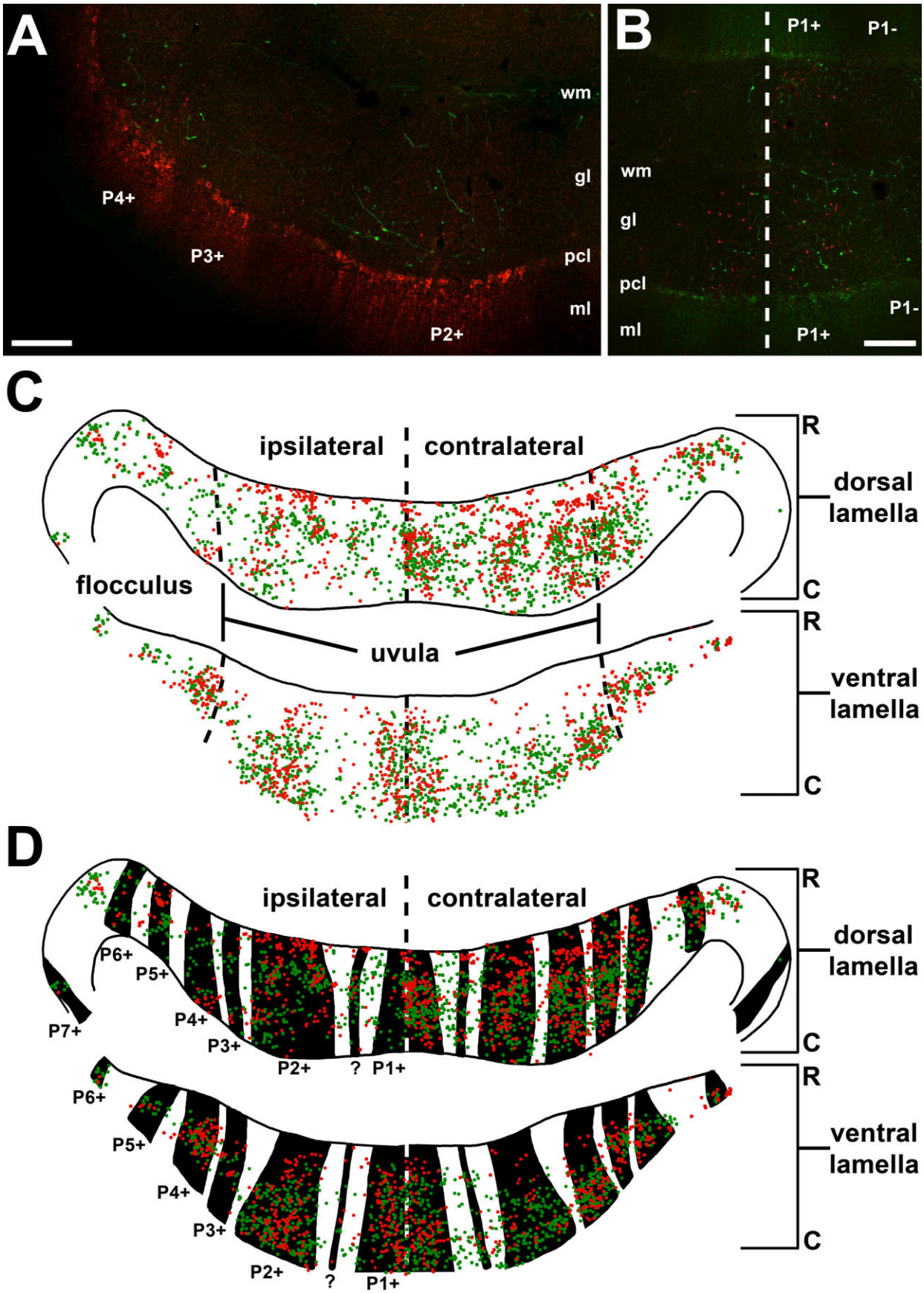
A
wm
gl
P4+
P3+
pcl
ml
P2+
B
P1+
P1-
wm
gl
pcl
ml
P1-
P1+
C
ipsilateral
contralateral
R
dorsal
lamella
C
flocculus
uvula
R
ventral
lamella
C
D
ipsilateral
contralateral
R
dorsal
lamella
C
P6+
P5+
P4+
P7+
P3+
P2+
?
P1+
R
ventral
lamella
C
P6+
P5+
P4+
P3+
P2+
?
P1+

Figure 8

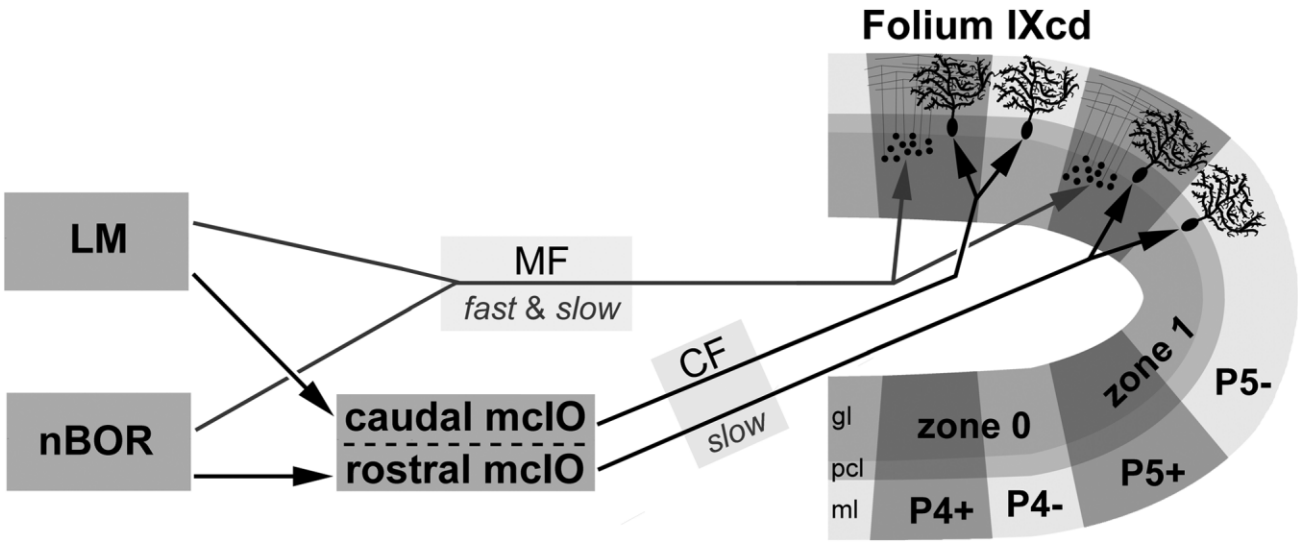

Figure 9. Optic flow input from the the nucleus lentiformis mesencephali (LM) and the nucleus of the basal optic root (nBOR) to the vestibulocerebellum (VbC) in pigeons. This schematic illustrates the visual afferents projecting to the flocculus (of folium IXcd) from the LM and nBOR. For simplicity, only floccular zones 0 and 1 are shown. The mossy fiber (MF) inputs originate from both *fast* and *slow* cells in the LM and nBOR, whereas the climbing fiber (CF) inputs via the medial column of the inferior olive (mcIO) originate primarily from *slow* cells in the LM and nBOR (see Winship et al., 2005). The MF pathway terminates in the granular cell layer in zebrin-immunopositive stripes (P4+ and P5+). The CF pathways terminate in parasagittal zones of a zebrin-immunopositive and -immunonegative pair (P4+/− and P5+/−), with the caudal mcIO projecting to the rVA responsive zones in the flocculus (zones 0) and the rostral mcIO projecting to the rH45 zones in the flocculus (zone 1). gl, granular layer; ml, molecular layer; Pcl, Purkinje cell layer; wm, cerebellar white matter.

cause there has been a lack of sufficient investigation into the anatomical interrelationship between these MF and CF systems, as well as the intrinsic biochemical properties of the Purkinje cells (Pijpers et al., 2006).

Recent investigations into the collateralization of CF and MF terminals in the cerebellum in relation to zebrin expression, in rats, have made great strides in determining the anatomical relationship between these systems (Ruigrok, 2003; Voogd et al., 2003; Pijpers et al., 2006). For example, Pijpers and colleagues (2006) investigated the collateral terminations of MFs and CFs from small retrograde tracer injections and correlated the resulting terminal pattern with zebrin stripes. They found that labeled MF collaterals generally distribute to the same lobules as CF collaterals and were always present in the granular layer directly subjacent to labeled CF collaterals. They also found that additional parasagittal clusters of MF terminals were labeled in other cerebellar regions, and these MF terminal zones often had the same zebrin signature as the source of the collateralization. They suggest that the various MF collateral zones, with the same zebrin expression characteristic, may be functionally linked. They also conclude that the MF and CF systems are closely aligned and that this is a consistent and widespread feature of cerebellar cortical organization.

In the pigeon VbC, the lack of sharp MF terminal boundaries and the fact that the relationship between visual MF afferents and zebrin expression seems to be more of a general pattern might suggest that, whereas the zebrin+ regions may share some underlying similarity in functional architecture with the visual MF terminal regions from the LM and nBOR, it is unlikely that the zebrin boundaries themselves are driving the organization of the MF projection pattern. Taken together with the zebrin correlation to the CF projection pattern observed in the pigeon flocculus (Pakan and Wylie, 2008), our results suggest a complicated organizational relationship between visual afferents and the intrinsic zebrin antigenic map in the VbC.

Figure 8. Reconstruction of MF terminals resulting from injections in the nucleus lentiformis mesencephali (LM) and the nucleus of the basal optic root (nBOR) from Case #5. A,B: Photomicrographs of the typical pattern of resulting MF terminals (rosettes) in folium IXcd from injections in the nBOR (green) and LM (red) and the zebrin expression. **A:** Note the correspondence between the zebrin-positive stripes (P2+ and P4+; red in Purkinje cell layer and molecular layer) and the MF terminals of the LM and nBOR in the granular layer. **B:** Region of folium IXcd directly surrounding the midline (dotted line) and the P1+ zebrin stripe (green in Purkinje cell layer and molecular layer); note the absence of MF terminal labeling in the ipsilateral dorsal lamella. gl, granular layer; ml, molecular layer; Pcl, Purkinje cell layer; wm, cerebellar white matter. See Figure 6 caption for details on **C** and **D**. A magenta-green copy of this figure is available as Supplementary Figure S6. Scale bar equals; 200 μm in A,B.

Functional implications for the control of compensatory eye and eye movements

It has been well established that the VbC is important for integrating visual, vestibular, and other sensorimotor information in producing compensatory head and eye movements (for reviews, see Simpson, 1984; Waespe and Henn, 1987; Voogd and Barmack, 2006). The functional implications of the findings of the present study (the organization of visual MF inputs to the zebrin stripes) are dependent on the actions of the granule-cell/parallel fibers on nearby Purkinje cells. A principle excitatory drive to a Purkinje cells arises from the synaptic contacts of ascending axons of granule cells that are directly subjacent to that Purkinje cell (Eccles et al., 1968; Brown and Bower, 2001; Lu et al., 2005). In this vein, the zebrin+ Purkinje cells in folium IXcd of the VbC would receive more excitatory visual MF input than the zebrin− Purkinje cells. In terms of the visual-vestibular interactions in mediating the vestibulo-ocular response, it is known that visual signals are especially useful at low head velocities, at which the vestibular response is quite sluggish (Wilson and Melvill Jones, 1979). That is, the zebrin+ Purkinje cells would be more active during low-frequency head movements. Also, at the onset of a visual stimulus there is a very brief period (50–100 ms) prior to any compensatory eye movement when retinal slip velocity is high (Collewijn, 1972), and again one might expect that the zebrin+ Purkinje cells would be preferentially active. However, the actions of granule cells on Purkinje cells via parallel fiber synapses and inhibitory interneurons cannot be discounted (Lu et al., 2005). Indeed, for the forelimb C3 region of the anterior lobe, Ekerot and Jorntell (2003) suggest that granule cells actually have a profound inhibitory influence through the actions of interneurons on directly adjacent Purkinje cells, and an excitatory influence on Purkinje cells in neighboring microzones (see also Garwicz et al., 1998; Ekerot and Jorntell, 2001, 2008; Jorntell and Ekerot, 2006). Therefore, the functional implication of these zonal MF patterns remains to be resolved.

Other mossy fiber inputs to folium IXcd

As the visual MFs project mainly to the zebrin+ regions in folium IXcd, the question arises as to which afferent MF inputs are projecting to the zebrin− regions. There are several other inputs to folium IXcd in birds, including: primary vestibular inputs (although these are mainly to folium X; Schwarz and Schwarz, 1983), secondary vestibular inputs (Brecha et al., 1980; Arends and Zeigler, 1991; Diaz and Puelles, 2003; Pakan et al., 2008), pontocerebellar inputs (Freedman et al., 1975), and spinocerebellar inputs (Vielvoye and Voogd, 1977; Okado et al., 1987; Necker, 1994). Using anterograde techniques, the topographic distribution of mossy fibers has been described only with respect to the spinocerebellar and pontocerbellar projections. Vielvoye (1977) described in detail the topography of the spinocerebellar projections in white leghorn chickens (*Gallus domesticus*). The spinocerebellar mossy fibers (and pontocerebellar mossy fibers; Freedman et al., 1975) tend to project to deeper portions of the granular layer, rather than superficially (i.e., subjacent to the Purkinje cell layer), as is the case for the LM and nBOR mossy fiber inputs. More importantly, there is a clear parasagittal distribution of mossy fiber terminals in IXcd, where there are several clusters (Vielvoye, 1977; Okado et al., 1987). How these clusters relate to the visual mossy fiber inputs and the zebrin stripes is yet to be determined.

CONCLUSIONS

From the results of the current study and our previous findings (Pakan and Wylie, 2008), a comprehensive picture of the visual MF and olivocerebellar inputs in relation to the zebrin stripes in the flocculus has emerged and is shown in schematic form in Figure 9. In folium IXcd of the pigeon flocculus, the functional units consist of two rVA zones (zones 0 and 2) and two rH45 zones (1 and 3), which receive input from the caudal and rostral mcIO, respectively. Each of these zones includes a zebrin+ and zebrin− stripe. The visual MF projections terminate in a parasagittal organization and generally cluster in the zebrin+ regions of each of these larger CF zones.

LITERATURE CITED

Ahn AH, Dziennis S, Hawkes R, Herrup K. 1994. The cloning of zebrin II reveals its identity with aldolase C. Development 120:2081–2090.

Akintunde A, Eisenman LM. 1994. External cuneocerebellar projection and Purkinje cell zebrin II bands: a direct comparison of parasagittal banding in the mouse cerebellum. J Chem Neuroanat 7:75–86.

Albus JS. 1971. A Theory on Cerebellar Function. Math Biosci 10:25–61.

Andersson G, Oscarsson O. 1978a. Climbing fiber microzones in cerebellar vermis and their projection to different groups of cells in the lateral vestibular nucleus. Exp Brain Res 32:565–579.

Andersson G, Oscarsson O. 1978b. Projections to lateral vestibular nucleus from cerebellar climbing fiber zones. Exp Brain Res 32:549–564.

Apps R, Garwicz M. 2005. Anatomical and physiological foundations of cerebellar information processing. Nat Rev Neurosci 6:297–311.

Arends J, Voogd J. 1989. Topographic aspects of the olivocerebellar system in the pigeon. Exp Brain Res Series 17:52–57.

Arends JJ, Zeigler HP. 1989. Cerebellar connections of the trigeminal system in the pigeon (*Columba livia*). Brain Res 487:69–78.

Arends JJ, Zeigler HP. 1991. Organization of the cerebellum in the pigeon (*Columba livia*): I. Corticonuclear and corticovestibular connections. J Comp Neurol 306:221–244.

Blanks RH, Precht W, Torigoe Y. 1983. Afferent projections to the cerebellar flocculus in the pigmented rat demonstrated by

retrograde transport of horseradish peroxidase. Exp Brain Res 52:293–306.
Brecha N, Karten HJ, Hunt SP. 1980. Projections of the nucleus of the basal optic root in the pigeon: an autoradiographic and horseradish peroxidase study. J Comp Neurol 189:615–670.
Brochu G, Maler L, Hawkes R. 1990. Zebrin II: a polypeptide antigen expressed selectively by Purkinje cells reveals compartments in rat and fish cerebellum. J Comp Neurol 291: 538–552.
Brown IE, Bower JM. 2001. Congruence of mossy fiber and climbing fiber tactile projections in the lateral hemispheres of the rat cerebellum. J Comp Neurol 429:59–70.
Burns S, Wallman J. 1981. Relation of single unit properties to the oculomotor function of the nucleus of the basal optic root (accessory optic system) in chickens. Exp Brain Res 42:171–180.
Cazin L, Magnin M, Lannou J. 1982. Non-cerebellar visual afferents to the vestibular nuclei involving the prepositus hypoglossal complex: an autoradiographic study in the rat. Exp Brain Res 48:309–313.
Clarke PG. 1977. Some visual and other connections to the cerebellum of the pigeon. J Comp Neurol 174:535–552.
Collewijn H. 1972. Latency and gain of the rabbit's optokinetic reactions to small movements. Brain Res 36:59–70.
Collewijn H. 1975. Direction-selective units in the rabbit's nucleus of the optic tract. Brain Res 100:489–508.
Crowder NA, Wylie DR. 2001. Fast and slow neurons in the nucleus of the basal optic root in pigeons. Neurosci Lett 304: 133–136.
Crowder NA, Winship IR, Wylie DR. 2000. Topographic organization of inferior olive cells projecting to translational zones in the vestibulocerebellum of pigeons. J Comp Neurol 419:87–95.
Crowder NA, Dawson MR, Wylie DR. 2003. Temporal frequency and velocity-like tuning in the pigeon accessory optic system. J Neurophysiol 90:1829–1841.
De Zeeuw CI, Wylie DR, DiGiorgi PL, Simpson JI. 1994. Projections of individual Purkinje cells of identified zones in the flocculus to the vestibular and cerebellar nuclei in the rabbit. J Comp Neurol 349:428–447.
Diaz C, Puelles L. 2003. Plurisegmental vestibulocerebellar projections and other hindbrain cerebellar afferents in midterm chick embryos: biotinylated dextranamine experiments in vitro. Neuroscience 117:71–82.
Eccles JC, Provini L, Strata P, Taborikova H. 1968. Analysis of electrical potentials evoked in the cerebellar anterior lobe by stimulation of hindlimb and forelimb nerves. Exp Brain Res 6:171–194.
Eisenman LM, Hawkes R. 1993. Antigenic compartmentation in the mouse cerebellar cortex: zebrin and HNK-1 reveal a complex, overlapping molecular topography. J Comp Neurol 335: 586–605.
Ekerot CF, Jorntell H. 2001. Parallel fibre receptive fields of Purkinje cells and interneurons are climbing fibre-specific. Eur J Neurosci 13:1303–1310.
Ekerot CF, Jorntell H. 2003. Parallel fiber receptive fields: a key to understanding cerebellar operation and learning. Cerebellum 2:101–109.
Ekerot CF, Jorntell H. 2008. Synaptic integration in cerebellar granule cells. Cerebellum 7:539–541.
Ekerot CF, Larson B. 1973. Correlation between sagittal projection zones of climbing and mossy fibre paths in cat cerebellar anterior lobe. Brain Res 64:446–450.
Finger TE, Karten HJ. 1978. The accessory optic system in teleosts. Brain Res 153:144–149.
Freedman SL, Feirabend HK, Vielvoye GJ, Voogd J. 1975. Reexamination of the ponto-cerebellar projection in the adult white leghorn (*Gallus domesticus*). Acta Morphol Neerl Scand 13:236–238.
Gamlin PD. 2006. The pretectum: connections and oculomotor-related roles. Prog Brain Res 151:379–405.
Gamlin PD, Cohen DH. 1988. Projections of the retinorecipient pretectal nuclei in the pigeon (*Columba livia*). J Comp Neurol 269:18–46.
Garwicz M, Jorntell H, Ekerot CF. 1998. Cutaneous receptive fields and topography of mossy fibres and climbing fibres projecting to cat cerebellar C3 zone. J Physiol 512:277–293.
Gerrits NM, Epema AH, Voogd J. 1984. The mossy fiber projection of the nucleus reticularis tegmenti pontis to the flocculus and adjacent ventral paraflocculus in the cat. Neuroscience 11: 627–644.
Gerrits NM, Voogd J, Nas WS. 1985. Cerebellar and olivary projections of the external and rostral internal cuneate nuclei in the cat. Exp Brain Res 57:239–255.
Gioanni H, Rey J, Villalobos J, Dalbera A. 1984. Single unit activity in the nucleus of the basal optic root (nBOR) during optokinetic, vestibular and visuo-vestibular stimulations in the alert pigeon (*Columba livia*). Exp Brain Res 57:49–60.
Giolli RA, Blanks RH, Torigoe Y. 1984. Pretectal and brain stem projections of the medial terminal nucleus of the accessory optic system of the rabbit and rat as studied by anterograde and retrograde neuronal tracing methods. J Comp Neurol 227: 228–251.
Giolli RA, Blanks RH, Torigoe Y, Williams DD. 1985. Projections of medial terminal accessory optic nucleus, ventral tegmental nuclei, and substantia nigra of rabbit and rat as studied by retrograde axonal transport of horseradish peroxidase. J Comp Neurol 232:99–116.
Giolli RA, Torigoe Y, Blanks RH, McDonald HM. 1988. Projections of the dorsal and lateral terminal accessory optic nuclei and of the interstitial nucleus of the superior fasciculus (posterior fibers) in the rabbit and rat. J Comp Neurol 277:608–620.
Giolli RA, Blanks RH, Lui F. 2006. The accessory optic system: basic organization with an update on connectivity, neurochemistry, and function. Prog Brain Res 151:407–440.
Gottlieb MD, McKenna OC. 1986. Light and electron microscopic study of an avian pretectal nucleus, the lentiform nucleus of the mesencephalon, magnocellular division. J Comp Neurol 248:133–145.
Graf W, Simpson JI, Leonard CS. 1988. Spatial organization of visual messages of the rabbit's cerebellar flocculus. II. Complex and simple spike responses of Purkinje cells. J Neurophysiol 60:2091–2121.
Grasse K, Cynader M. 1990. The accessory optic system in frontal-eyed animals. In: Leventhal A, editor. Vision and visual dysfunction,vol. IV. The neuronal basis of visual function. New York: MacMillan. p 111–139.
Gravel C, Hawkes R. 1990. Parasagittal organization of the rat cerebellar cortex: direct comparison of Purkinje cell compartments and the organization of the spinocerebellar projection. J Comp Neurol 291:79–102.
Haines DE, Sowa TE. 1985. Evidence of a direct projection from the medial terminal nucleus of the accessory optic system to lobule IX of the cerebellar cortex in the tree shrew (*Tupaia glis*). Neurosci Lett 55:125–130.
Hawkes R. 1992. Antigenic markers of cerebellar modules in the adult mouse. Biochem Soc Trans 20:391–395.
Hawkes R, Gravel C. 1991. The modular cerebellum. Prog Neurobiol 36:309–327.
Hawkes R, Herrup K. 1995. Aldolase C/zebrin II and the regionalization of the cerebellum. J Mol Neurosci 6:147–158.
Hawkes R, Blyth S, Chockkan V, Tano D, Ji Z, Mascher C. 1993. Structural and molecular compartmentation in the cerebellum. Can J Neurol Sci 20(Suppl 3):S29–35.

Herrup K, Kuemerle B. 1997. The compartmentalization of the cerebellum. Annu Rev Neurosci 20:61–90.
Hoffmann KP, Schoppmann A. 1975. Retinal input to direction selective cells in the nucleus tractus opticus of the cat. Brain Res 99:359–366.
Holstege G, Collewijn H. 1982. The efferent connections of the nucleus of the optic tract and the superior colliculus in the rabbit. J Comp Neurol 209:139–175.
Ito M. 1984. The cerebellum and neural control. New York: Raven.
Itoh K. 1977. Efferent projections of the pretectum in the cat. Exp Brain Res 30:89–105.
Iwaniuk AN, Marzban H, Pakan JM, Watanabe M, Hawkes R, Wylie DR. 2009. Compartmentation of the cerebellar cortex of hummingbirds (Aves: Trochilidae) revealed by the expression of zebrin II and phospholipase C beta 4. J Chem Neuroanat 37: 55–63.
Ji Z, Hawkes R. 1994. Topography of Purkinje cell compartments and mossy fiber terminal fields in lobules II and III of the rat cerebellar cortex: spinocerebellar and cuneocerebellar projections. Neuroscience 61:935–954.
Jorntell H, Ekerot CF. 2006. Properties of somatosensory synaptic integration in cerebellar granule cells in vivo. J Neurosci 26:11786–11797.
Karten H, Hodos W. 1967. A stereotaxic atlas of the brain of the pigeon (*Columba livia*). Baltimore, MD: Johns Hopkins Press.
Kawasaki T, Sato Y. 1980. Afferent projection from the dorsal nucleus of the raphe to the flocculus in cats. Brain Res 197: 496–502.
Langer T, Fuchs AF, Scudder CA, Chubb MC. 1985. Afferents to the flocculus of the cerebellum in the rhesus macaque as revealed by retrograde transport of horseradish peroxidase. J Comp Neurol 235:1–25.
Larouche M, Hawkes R. 2006. From clusters to stripes: the developmental origins of adult cerebellar compartmentation. Cerebellum 5:77–88.
Larsell O. 1967. The cerebellum: from myxinoids through birds. Jansen J, editor. Minneapolis, MN: The University of Minnesota Press.
Lau KL, Glover RG, Linkenhoker B, Wylie DR. 1998. Topographical organization of inferior olive cells projecting to translation and rotation zones in the vestibulocerebellum of pigeons. Neuroscience 85:605–614.
Llinas R, Sasaki K. 1989. The functional organization of the olivocerebellar system as examined by multiple Purkinje cell recordings. Eur J Neurosci 1:587–602.
Lu H, Hartmann MJ, Bower JM. 2005. Correlations between purkinje cell single-unit activity and simultaneously recorded field potentials in the immediately underlying granule cell layer. J Neurophysiol 94:1849–1860.
Maekawa K, Takeda T. 1976. Electrophysiological identification of the climbing and mossy fiber pathways from the rabbit's retina to the contralateral cerebellar flocculus. Brain Res 109: 169–174.
Marr D. 1969. A theory of cerebellar cortex. J Physiol 202:437–470.
Matsushita M, Tanami T, Yaginuma H. 1984. Differential distribution of spinocerebellar fiber terminals within the lobules of the cerebellar anterior lobe in the cat: an anterograde WGA-HRP study. Brain Res 305:157–161.
Matsushita M, Ragnarson B, Grant G. 1991. Topographic relationship between sagittal Purkinje cell bands revealed by a monoclonal antibody to zebrin I and spinocerebellar projections arising from the central cervical nucleus in the rat. Exp Brain Res 84:133–141.
McKenna OC, Wallman J. 1985. Accessory optic system and pretectum of birds: comparisons with those of other vertebrates. Brain Behav Evol 26:91–116.
Mizuno N, Mochizuki K, Akimoto C, Matsushima R. 1973. Pretectal projections to the inferior olive in the rabbit. Exp Neurol 39:498–506.
Montgomery N, Fite KV, Bengston L. 1981. The accessory optic system of *Rana pipiens*: neuroanatomical connections and intrinsic organization. J Comp Neurol 203:595–612.
Morgan B, Frost BJ. 1981. Visual response characteristics of neurons in nucleus of basal optic root of pigeons. Exp Brain Res 42:181–188.
Mustari MJ, Fuchs AF, Kaneko CR, Robinson FR. 1994. Anatomical connections of the primate pretectal nucleus of the optic tract. J Comp Neurol 349:111–128.
Nagao S, Kitamura T, Nakamura N, Hiramatsu T, Yamada J. 1997. Differences of the primate flocculus and ventral paraflocculus in the mossy and climbing fiber input organization. J Comp Neurol 382:480–498.
Necker R. 1994. Sensorimotor aspects of flight control in birds: specializations in the spinal cord. Eur J Morphol 32:207–211.
Okado N, Ito R, Homma S. 1987. The terminal distribution pattern of spinocerebellar fibers. An anterograde labelling study in the posthatching chick. Anat Embryol (Berl) 176:175–182.
Oscarsson O. 1969. Termination and functional organization of the dorsal spino-olivocerebellar path. J Physiol 200:129–149.
Ozol KO, Hawkes R. 1997. Compartmentation of the granular layer of the cerebellum. Histol Histopathol 12:171–184.
Ozol K, Hayden JM, Oberdick J, Hawkes R. 1999. Transverse zones in the vermis of the mouse cerebellum. J Comp Neurol 412:95–111.
Pakan JM, Wylie DR. 2006. Two optic flow pathways from the pretectal nucleus lentiformis mesencephali to the cerebellum in pigeons (*Columba livia*). J Comp Neurol 499:732–744.
Pakan JM, Wylie DR. 2008. Congruence of zebrin II expression and functional zones defined by climbing fiber topography in the flocculus. Neuroscience 157:57–69.
Pakan JM, Todd KG, Nguyen AP, Winship IR, Hurd PL, Jantzie LL, Wylie DR. 2005. Inferior olivary neurons innervate multiple zones of the flocculus in pigeons (*Columba livia*). J Comp Neurol 486:159–168.
Pakan JM, Krueger K, Kelcher E, Cooper S, Todd KG, Wylie DR. 2006. Projections of the nucleus lentiformis mesencephali in pigeons (*Columba livia*): a comparison of the morphology and distribution of neurons with different efferent projections. J Comp Neurol 495:84–99.
Pakan JM, Iwaniuk AN, Wylie DR, Hawkes R, Marzban H. 2007. Purkinje cell compartmentation as revealed by zebrin II expression in the cerebellar cortex of pigeons (*Columba livia*). J Comp Neurol 501:619–630.
Pakan JM, Graham DJ, Iwaniuk AN, Wylie DR. 2008. Differential projections from the vestibular nuclei to the flocculus and uvula-nodulus in pigeons (*Columba livia*). J Comp Neurol 508: 402–417.
Pijpers A, Voogd J, Ruigrok TJ. 2005. Topography of olivo-corticonuclear modules in the intermediate cerebellum of the rat. J Comp Neurol 492:193–213.
Pijpers A, Apps R, Pardoe J, Voogd J, Ruigrok TJ. 2006. Precise spatial relationships between mossy fibers and climbing fibers in rat cerebellar cortical zones. J Neurosci 26):12067–12080.
Reiner A, Karten HJ. 1978. A bisynaptic retinocerebellar pathway in the turtle. Brain Res 150:163–169.
Ruigrok TJ. 2003. Collateralization of climbing and mossy fibers projecting to the nodulus and flocculus of the rat cerebellum. J Comp Neurol 466:278–298.
Sato Y, Kawasaki T. 1991. Identification of the Purkinje cell/climbing fiber zone and its target neurons responsible for eye-movement control by the cerebellar flocculus. Brain Res Brain Res Rev 16:39–64.

Sato Y, Kawasaki T, Ikarashi K. 1983. Afferent projections from the brainstem to the three floccular zones in cats. II. Mossy fiber projections. Brain Res 272:37–48.

Schonewille M, Luo C, Ruigrok TJ, Voogd J, Schmolesky MT, Rutteman M, Hoebeek FE, De Jeu MT, De Zeeuw CI. 2006. Zonal organization of the mouse flocculus: physiology, input, and output. J Comp Neurol 497:670–682.

Schwarz IE, Schwarz DW. 1983. The primary vestibular projection to the cerebellar cortex in the pigeon (*Columba livia*). J Comp Neurol 216:438–444.

Serapide MF, Panto MR, Parenti R, Zappala A, Cicirata F. 2001. Multiple zonal projections of the basilar pontine nuclei to the cerebellar cortex of the rat. J Comp Neurol 430:471–484.

Serapide MF, Parenti R, Panto MR, Zappala A, Cicirata F. 2002. Multiple zonal projections of the nucleus reticularis tegmenti pontis to the cerebellar cortex of the rat. Eur J Neurosci 15: 1854–1858.

Sillitoe RV, Hawkes R. 2002. Whole-mount immunohistochemistry: a high-throughput screen for patterning defects in the mouse cerebellum. J Histochem Cytochem 50:235–244.

Sillitoe RV, Marzban H, Larouche M, Zahedi S, Affanni J, Hawkes R. 2005. Conservation of the architecture of the anterior lobe vermis of the cerebellum across mammalian species. Prog Brain Res 148:283–297.

Simpson JI. 1984. The accessory optic system. Annu Rev Neurosci 7:13–41.

Simpson JI, Giolli RA, Blanks RH. 1988. The pretectal nuclear complex and the accessory optic system. Rev Oculomot Res 2:335–364.

Sugihara I. 2006. Organization and remodeling of the olivocerebellar climbing fiber projection. Cerebellum 5:15–22.

Sugihara I, Quy PN. 2007. Identification of aldolase C compartments in the mouse cerebellar cortex by olivocerebellar labeling. J Comp Neurol 500:1076–1092.

Sugihara I, Shinoda Y. 2004. Molecular, topographic, and functional organization of the cerebellar cortex: a study with combined aldolase C and olivocerebellar labeling. J Neurosci 24: 8771–8785.

Sugihara I, Shinoda Y. 2007. Molecular, topographic, and functional organization of the cerebellar nuclei: analysis by three-dimensional mapping of the olivonuclear projection and aldolase C labeling. J Neurosci 27:9696–9710.

Sugihara I, Ebata S, Shinoda Y. 2004. Functional compartmentalization in the flocculus and the ventral dentate and dorsal group y nuclei: an analysis of single olivocerebellar axonal morphology. J Comp Neurol 470:113–133.

Takeda T, Maekawa K. 1976. The origin of the pretecto-olivary tract. A study using the horseradish peroxidase method. Brain Res 117:319–325.

Terasawa K, Otani K, Yamada J. 1979. Descending pathways of the nucleus of the optic tract in the rat. Brain Res 173:405417.

Torigoe Y, Blanks RH, Precht W. 1986a. Anatomical studies on the nucleus reticularis tegmenti pontis in the pigmented rat. I. Cytoarchitecture, topography, and cerebral cortical afferents. J Comp Neurol 243:7187.

Torigoe Y, Blanks RH, Precht W. 1986b. Anatomical studies on the nucleus reticularis tegmenti pontis in the pigmented rat. II. Subcortical afferents demonstrated by the retrograde transport of horseradish peroxidase. J Comp Neurol 243:88105.

Vielvoye GJ. 1977. Spinocerebellar tracts in the white Leghorn (*Gallus domesticus*). Leiden: Rijksuniversiteit te Leiden. 181 p.

Vielvoye GJ, Voogd J. 1977. Time dependence of terminal degeneration in spino-cerebellar mossy fiber rosettes in the chicken and the application of terminal degeneration in successive degeneration experiments. J Comp Neurol 175:233–242.

Voogd J. 1967. Comparative aspects of the structure and fibre connexions of the mammalian cerebellum. Prog Brain Res 25:94–134.

Voogd J, Barmack NH. 2006. Oculomotor cerebellum. Prog Brain Res 151:231–268.

Voogd J, Bigaré F. 1980. Topographical distribution of olivary and cortico nuclear fibers in the cerebellum: a review. In: The inferior olivary nucleus: anatomy and physiology. Courville J, de Montigny C, Lamarre Y, editors. New York: Raven. p 207–234.

Voogd J, Glickstein M. 1998. The anatomy of the cerebellum. Trends Neurosci 21:370–375.

Voogd J, Ruigrok TJ. 2004. The organization of the corticonuclear and olivocerebellar climbing fiber projections to the rat cerebellar vermis: the congruence of projection zones and the zebrin pattern. J Neurocytol 33:5–21.

Voogd J, Wylie DR. 2004. Functional and anatomical organization of floccular zones: a preserved feature in vertebrates. J Comp Neurol 470:107–112.

Voogd J, Broere G, van Rossum J. 1969. The medio-lateral distribution of the spinocerebellar projection in the anterior lobe and the simple lobule in the cat and a comparison with some other afferent fibre systems. Psychiatr Neurol Neurochir 72: 137–151.

Voogd J, Gerrits NM, Ruigrok TJ. 1996. Organization of the vestibulocerebellum. Ann N Y Acad Sci 781:553–579.

Voogd J, Pardoe J, Ruigrok TJ, Apps R. 2003. The distribution of climbing and mossy fiber collateral branches from the copula pyramidis and the paramedian lobule: congruence of climbing fiber cortical zones and the pattern of zebrin banding within the rat cerebellum. J Neurosci 23:4645–4656.

Wadiche JI, Jahr CE. 2005. Patterned expression of Purkinje cell glutamate transporters controls synaptic plasticity. Nat Neurosci 8:1329–1334.

Waespe W, Henn V. 1987. Gaze stabilization in the primate. The interaction of the vestibulo-ocular reflex, optokinetic nystagmus, and smooth pursuit. Rev Physiol Biochem Pharmacol 106:37–125.

Weber AE, Martin J, Ariel M. 2003. Connectivity of the turtle accessory optic system. Brain Res 989:76–90.

Welsh JP, Yuen G, Placantonakis DG, Vu TQ, Haiss F, O'Hearn E, Molliver ME, Aicher SA. 2002. Why do Purkinje cells die so easily after global brain ischemia? Aldolase C, EAAT4, and the cerebellar contribution to posthypoxic myoclonus. Adv Neurol 89:331–359.

Wilson J, Melvill Jones G. 1979. Mammalian vestibular physiology. New York: Plenum Press.

Winfield JA, Hendrickson A, Kimm J. 1978. Anatomical evidence that the medial terminal nucleus of the accessory optic tract in mammals provides a visual mossy fiber input to the flocculus. Brain Res 151:175–182.

Winship IR, Wylie DR. 2001. Responses of neurons in the medial column of the inferior olive in pigeons to translational and rotational optic flowfields. Exp Brain Res 141:63–78.

Winship IR, Wylie DR. 2003. Zonal organization of the vestibulocerebellum in pigeons (*Columba livia*): I. Climbing fiber input to the flocculus. J Comp Neurol 456:127–139.

Winship IR, Hurd PL, Wylie DR. 2005. Spatiotemporal tuning of optic flow inputs to the vestibulocerebellum in pigeons: differences between mossy and climbing fiber pathways. J Neurophysiol 93:1266–1277.

Winship IR, Crowder NA, Wylie DR. 2006. Quantitative reassessment of speed tuning in the accessory optic system and pretectum of pigeons. J Neurophysiol 95:546–551.

Winterson BJ, Brauth SE. 1985. Direction-selective single units in the nucleus lentiformis mesencephali of the pigeon (*Columba livia*). Exp Brain Res 60:215–226.

Wylie DR. 2001. Projections from the nucleus of the basal optic root and nucleus lentiformis mesencephali to the inferior olive in pigeons (*Columba livia*). J Comp Neurol 429:502–513.

Wylie DR, Crowder NA. 2000. Spatiotemporal properties of fast and slow neurons in the pretectal nucleus lentiformis mesencephali in pigeons. J Neurophysiol 84:2529–2540.

Wylie DR, Frost BJ. 1990. The visual response properties of neurons in the nucleus of the basal optic root of the pigeon: a quantitative analysis. Exp Brain Res 82:327–336.

Wylie DR, Frost BJ. 1991. Purkinje cells in the vestibulocerebellum of the pigeon respond best to either translational or rotational wholefield visual motion. Exp Brain Res 86:229–232.

Wylie DR, Frost BJ. 1993. Responses of pigeon vestibulocerebellar neurons to optokinetic stimulation. II. The 3-dimensional reference frame of rotation neurons in the flocculus. J Neurophysiol 70:2647–2659.

Wylie DR, Frost BJ. 1996. The pigeon optokinetic system: visual input in extraocular muscle coordinates. Vis Neurosci 13: 945–953.

Wylie DR, Frost BJ. 1999. Complex spike activity of Purkinje cells in the ventral uvula and nodulus of pigeons in response to translational optic flow. J Neurophysiol 81:256–266.

Wylie DR, Linkenhoker B. 1996. Mossy fibres from the nucleus of the basal optic root project to the vestibular and cerebellar nuclei in pigeons. Neurosci Lett 219:83–86.

Wylie DR, Kripalani T, Frost BJ. 1993. Responses of pigeon vestibulocerebellar neurons to optokinetic stimulation. I. Functional organization of neurons discriminating between translational and rotational visual flow. J Neurophysiol 70:2632–2646.

Wylie DR, De Zeeuw CI, DiGiorgi PL, Simpson JI. 1994. Projections of individual Purkinje cells of identified zones in the ventral nodulus to the vestibular and cerebellar nuclei in the rabbit. J Comp Neurol 349:448–463.

Wylie DR, De Zeeuw CI, Simpson JI. 1995. Temporal relations of the complex spike activity of Purkinje cell pairs in the vestibulocerebellum of rabbits. J Neurosci 15:2875–2887.

Wylie DR, Linkenhoker B, Lau KL. 1997. Projections of the nucleus of the basal optic root in pigeons (*Columba livia*) revealed with biotinylated dextran amine. J Comp Neurol 384: 517–536.

Wylie DR, Bischof WF, Frost BJ. 1998. Common reference frame for neural coding of translational and rotational optic flow. Nature 392:278–282.

Wylie DR, Lau KL, Lu X, Glover RG, Valsangkar-Smyth M. 1999a. Projections of purkinje cells in the translation and rotation zones of the vestibulocerebellum in pigeon (*Columba livia*). J Comp Neurol 413:480–493.

Wylie DR, Winship IR, Glover RG. 1999b. Projections from the medial column of the inferior olive to different classes of rotation-sensitive Purkinje cells in the flocculus of pigeons. Neurosci Lett 268:97–100.

Wylie DR, Brown MR, Barkley RR, Winship IR, Crowder NA, Todd KG. 2003a. Zonal organization of the vestibulocerebellum in pigeons (*Columba livia*): II. Projections of the rotation zones of the flocculus. J Comp Neurol 456:140–153.

Wylie DR, Brown MR, Winship IR, Crowder NA, Todd KG. 2003b. Zonal organization of the vestibulocerebellum in pigeons (*Columba livia*): III. Projections of the translation zones of the ventral uvula and nodulus. J Comp Neurol 465:179–194.

Wylie DR, Pakan JM, Elliott CA, Graham DJ, Iwaniuk AN. 2007. Projections of the nucleus of the basal optic root in pigeons (*Columba livia*): a comparison of the morphology and distribution of neurons with different efferent projections. Vis Neurosci 24:691–707.